VŠB – Technical University of Ostrava
Faculty of Electrical Engineering and Computer Science
Department of Telecommunications

Study of Optical Properties of the Milk Material Used in the Automotive Industry

Studium optických vlastností mléčných materiálů používaných v automobilovém průmyslu

2016 Bc. Michal Miček

VŠB - Technical University of Ostrava
Faculty of Electrical Engineering and Computer Science
Department of Telecommunications

Diploma Thesis Assignment

Student: **Bc. Michal Miček**

Study Programme: N2647 Information and Communication Technology

Study Branch: 2601T013 Telecommunication Technology

Title: Study of Optical Properties of the Milk Material Used in the Automotive Industry
Studium optických vlastností mléčných materiálů používaných v automobilovém průmyslu

The thesis language: English

Description:

With increasing demand for modern technologies and their utilization even the companies involved in automotive industry have started development of new headlamp types. The aim of their effort is to get headlamps providing high quality of luminance color rendering for human sight and also lighting quality sufficient enough for different types of headlamps.
The goal of this diploma thesis is study of very interesting material used in automotive industry in form of so called milk material. This material has very interesting optical properties that are necessary to study closely before it can be used in headlamps of a car. Student's task will be preparation of background research in the field of transparent materials utilization in automotive industry and to perform a simulation in the LightTools software application with comparison of optical properties of individual materials.

1. Describe optical properties of milk materials used in automotive industry.
2. Compare differences in optical properties between usual transparent materials used in automotive industry (PMMA/PC) and milk material.
3. Design an optical system from milk material that will be able to align a light to the required directions.
4. Simulate designed optical system in the LightTools software and perform an evaluation of obtained results.

References:

[1] SOKANSKÝ, Karel, Tomáš NOVÁK, Marek BÁLSKÝ, Zdeněk BLÁHA, Zbyněk CARBOL, Daniel DIVIŠ, Blahoslav SOCHA, Jaroslav ŠNOBL, Jan ŠUMPICH a Petr ZÁVADA. *Světelná technika*. Vyd. 1. Praha: České vysoké učení technické v Praze, 2011, 255 s. ISBN 978-80-01-04941-9.
[2] BAXANT, P. Zdroje LED v osvětlovací technice. Electro, 2011, roč. 21, č. 5, s. 6-9. ISSN: 1210- 0889
[3] HALLIDAY, D, RESNICK, R, WALKER, J. Fyzika. 1997. vyd.: VUTIUM, 2001. 1254 s. ISBN 80-214-1868-0.
[4] SCHUBERT, E. Fred. Light-Emitting Diodes. 2003. vyd.:Cambridge University Press, 432 s. ISBN 978-0-521-86538-8.

Extent and terms of a thesis are specified in directions for its elaboration that are opened to the public on the web sites of the faculty.

Supervisor: **Ing. Jan Látal**

Date of issue: 01.09.2014

Date of submission: 29.04.2016

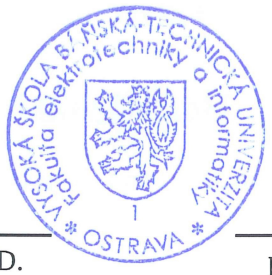

doc. Ing. Miroslav Vozňák, Ph.D.
Head of Department

prof. RNDr. Václav Snášel, CSc.
Dean of Faculty

I hereby declare that this master's thesis was written by myself. I have quoted all the references I have drawn upon.

Ostrava, 25 April 2016 .....

I hereby agree to the publishing of the master's thesis as per s. 26, ss. 9 of the Study and Examination Regulations for Master's Degree Programmes at VŠB – Technical University of Ostrava.

Ostrava, 25 April 2016 M. KRIZAK .....

I would like to express my gratitude to my supervisor Ing. Jan Látal for the useful comments, remarks and engagement through the learning process of this master thesis. Furthermore I would like to thank Ing. Patrik Hanulák for introducing me to the topic as well for the support on the way. Also, I like to thank Bc. Zuzana Vančová and Ing. Aleš Roszoha. And last but not least, I would like to thank my loved ones, who have supported me throughout entire studies.

Abstract

The aim of this thesis is to study a progressive material used in the automotive industry in form of so called Milky material. The thesis provides theoretical background of this material which needs to be studied in depth before it can be used in the automotive headlamps. The study also deals with the description of basic optical phenomena and the principles used in the automotive lighting. The practical part of this thesis is dedicated to the simulations testing the optical properties of Milky and transparent materials as well as a comparison between them. This thesis includes design and simulation of the optical system made from Milky material that is able to align a light to the required direction.

Key Words: Milky material, PMMA, PC, automotive lighting, geometrical optics, volume scattering

Contents

List of symbols and abbreviations

cd	–	Candela
CIE	–	Commission Internationale de l'Éclairage
DC	–	Direct Current
ECE	–	Economic Commission for Europe
InGaN	–	Indium Gallium Nitrid
K	–	Kelvin
LED	–	Light Emitting Diode
lm	–	Lumen
lx	–	Lux
OLED	–	Organic Light-Emitting Diode
PC	–	Polycarbonate
PCB	–	Printed Circuit Board
PMMA	–	Polymethylmethacrylate
RGB	–	Red-Green-Blue
SI	–	The International System of Units
sqm	–	Square Meters
UV	–	Ultraviolet
YAG	–	Yttrium Aluminum Garnet

List of Figures

List of Tables

Introduction

With regard to the increasing demand for modern technologies and their utilization, the companies involved in automotive industry have started to develop a new headlamp type. The aim of their effort is to get headlamps providing high quality of luminance colour rendering for human sight and also lighting quality sufficient enough for different types of headlamps.

The aim of this thesis is to study very remarkable material used in automotive industry in form of so called Milky material. This material has very interesting optical properties that need to be studied thoroughly before they can be used in car's headlamps. Therefore, the aim of this thesis is prepare a background research in the field of the transparent materials utilization in automotive industry as well as to perform a simulation in the LightTools software application with comparison of optical properties of individual materials. The thesis is prepared for the company Varroc Lighting Systems which is the global automotive supplier specializing in a concept design, research & development and manufacturing of the exterior lighting products such as headlamps, signal lamps, auxiliary lamps, projector systems and electronic control modules.

The paper includes two main parts - theoretical and practical part. Theoretical part deals with the basic phenomena, principles and properties of the transparent and Milky material. Practical part is dedicated to the processes of simulations in the LightTools software application. In this part will be simulated individual materials and evaluated optical properties, afterwards the differences between them will be described.

The thesis is divided into nine chapters, excluding introduction. The second chapter focuses on the properties of the diffuse polymers (Milky materials) used in the automotive industry. This chapter also includes basic information about other progressive trends in the automotive industry such as LED and OLED technologies and Laser light for headlights. The third chapter deals with the photometry in the automotive lighting. It contains description of the basic photometric quantities (Luminous flux, Luminous Intensity, Illuminance and Luminance). The fourth chapter is dedicated to description of the photometric measurement in the automotive lighting. In this chapter is described measurement of the photometry serving as a validation of product and measurement of luminance which is also significant with increasing demand on design of automotive lighting.

The fifth chapter focuses on Colorimetry and its function in automotive. This chapter includes explanation of normalized photopic and scotopic function as well as definition of CIE XYZ colour space. The colours of the individual lighting function and their definitions are also mentioned in this chapter. In sixth chapter are described basic optical phenomena and principles used in automotive lighting such as Refractive index, Law of reflection and refraction, Snell's law, Critical angle and Total internal reflection. Part of this chapter is also dedicated to the description of the basic optical element (Mirror, Lense, Prism, Collimator) which are often used in the automotive lighting. The seventh chapter deals with Volume scattering – the main

phenomena causing diffuse effect in Milky materials. This chapter contains the short description of general theory of this scattering and description of Multiple scattering.

The last two chapters are concern the practical part of this thesis. The eighth chapter describes process of simulations of various optical elements made from Milky and transparent materials as well as their comparison. The ninth chapter is dedicated to the simulation of proposed optical system from Milky material allowing aligning the light to the required direction. The last chapter indicates the evaluation of obtained results, difficulties during the project and ideas for further development.

1 Trends in automotive lighting

Since the invention of the automobile, lighting has been an important subsystem on all ground vehicles. Nowadays, automotive lighting passes through dynamic development of light sources technologies, as well as advanced development and improvement of constructions of headlamps and signal lamps. The emphasis is placed on increasing active and passive safety, thus on two important features in outer automotive lighting - to see and be seen. Original claims to functionality of lighting and signaling have been adapted to new requirements directed to minimizing the cost of production and development, durability of materials, as well as environmental protection. The technology used in automotive lighting has rapidly expanded to make lighting more value added, safer and more pleasant to customers.

Last but not least, important requirements for automotive lighting are aesthetic and design demands. Automotive manufacturers have always used distinctive styling to differentiate their vehicles. Advances in lighting technologies allow them to create a unique "signature", that gives overall face and appearance of vehicle and it is vital to keep up.

Figure 1: Design signatures: Range Rover Evoque (left), Skoda C-shape motive (right)

The aim is to create lighting, which is able to provide maximum possible lighting condition within legislation and applicable standards and also to offer unique stylistic feature. It means that automotive light has to fulfill four main conditions. It must meets legal requirements, must give the impression, be attractive and be recognizable from others.

With increasing demands on the stylistic function of lighting and using new light sources such as LED, very important factor for lighting is uniform distribution of light, called homogeneity. As is well known, LEDs are point sources and one of the disadvantages associated with these sources is the unpleasant hot spot effect typically generated by these light sources. Due to these facts, has to be used some kind of technique, which helps to eliminate hot spot phenomenon, and ensure that light becomes homogenous.

There are two techniques to achieve light scattering. The material can be made from frosted glass, with irregular structured surface. The size of grain is approximately $10\,\mu m$ and this technique can scatter light due to refraction. Alternatively, material can be made from translucent resin, which contains appropriate additives. Diffusion strength and transmission depend greatly on the type and concentration of additive. This kind of thermoplastic polymer is called Milky material and uses scattering effect within the medium. Diffusing polymers have many bene-

fits compared to other scattering techniques, and are increasingly used in automotive lighting. Detailed description of this material is in the following subsection.

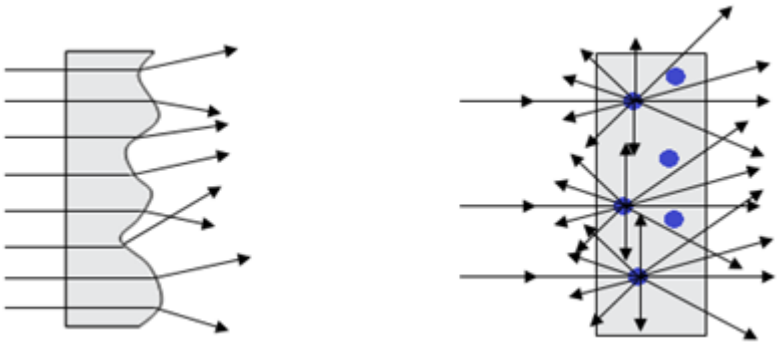

Figure 2: Techniques how to achieve diffuse lights in automotive: Graining: used for maintaining non lit appearance (left); Diffuse polymers-Milky materials (right)

1.1 Diffuse polymers

Plastics are rapidly updating car lighting systems. Glass lights lenses have been practically replaced by transparent polymers. However, with increasing demands on homogeneity of light, especially in rear lamps is more often used new kind of thermoplastic material - diffuse polymer, so called Milky material. Diffuse polymers offer unique set of properties such as better diffusion of LED point light sources to provide even illumination. These materials have several advantages. The main advantage is that they are relative inexpensive. An additional benefit of this technology is that it is very customizable. Unlike fixed patterns or frosted lenses, can be molded into almost any shape. This gives car designers and engineers far more flexibility in styling and placement of lights.[1]

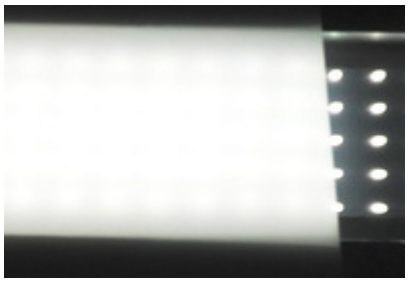

Figure 3: Diffuse polymers

Milky materials are made from transparent resin containing fine particles known as light diffusers. The size and shape of these particles, which is proprietary, makes this technology possible. Diffusivity of material largely depends on the difference in refractive index between particle and matrix, and the diameter of light diffuser agent. On the other side, more pure

the base resin, the better overall light transmittance of material. The main principle of diffuser polymers is that light passing through material softly bends around particles - diffusers. Consequently, light is dispersed in varied, mostly forward directions, while high overall light transmission is maintained. The final effect is overall wider distribution of light. The most of light waves bend a little - some more widely and others inward. A very small portion of light is blocked, reflected or absorbed. [2]

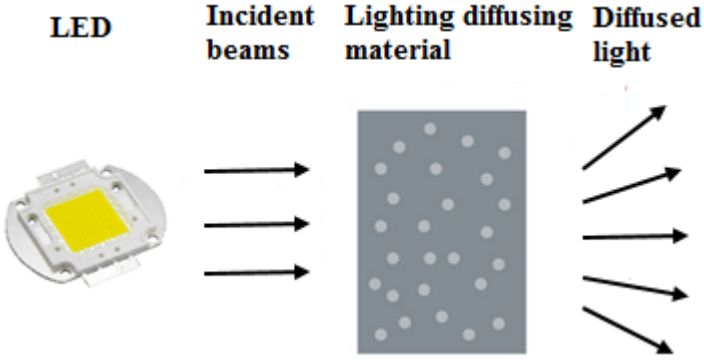

Figure 4: Principle of diffused light

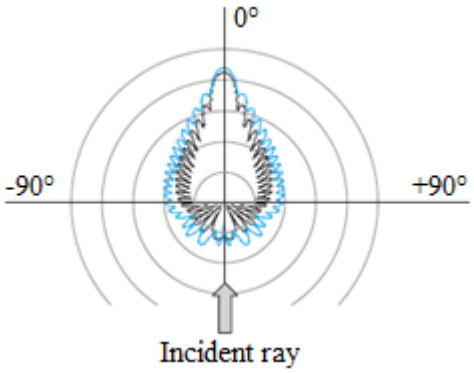

Figure 5: Mie scattering diagrams of two particles with different refractive indices. n of matrix is 1.50, n of particle is 1.55 and 1.60 for black line and blue line, respectively [3]

Assuming that the shape of a light diffuser particle is spherical, the diffusing performance due to a single diffuser agent particle can be determined by using the Mie scattering theory. Figure 5 shows example of angular dependence of scattered light. In this case, the particle diameter is the same but their refractive indices are different. As shown in figure, intensity of scattered light in forward direction is approximately the same, while the intensity at wider angles and back scattering are much stronger for particles with a larger refractive index difference compared to those with smaller refractive index difference [3]. Due to the reason, that diffusing agent particles are not single particles, the effect of multiple scattering must be considered. Therefore, accurately predicting light scattering characteristics for diffuser materials is quite difficult. The

effect of multiple scattering and volume scattering, main phenomenon that cause diffuse effect are detailed described in chapter 6.

The main materials for diffusing technology in automotive lighting available today are based on polymethylmethacrylate (PMMA) and polycarbonate (PC), although the same effects can be obtained on all transparent polymers [2]. The materials based on PMMA stand out for their optical and UV resistant properties, while the polycarbonate grades are particularly suited for applications requiring greater resilience and superior thermal properties. In automotive lighting polycarbonate is used for designing headlamps. On the other hand, PMMA materials are mostly used in rear-lamp designing .

For determination of diffusing properties of diffuser plates are usually used parameters such as diffusion factor, total light transmittance, hiding power and half angle value. Total light transmittance is a ratio of the light transmitted in forward direction and incident light. The diffusion factor represents homogeneity of diffusion and it is value determined from angular dependence of transmitted scattered light when the diffuser plate is illuminated with collimated light from perpendicular direction. The equation 2 determines the diffusion factor using intensity at 5, 20 and 70 degree. [5]

$$D = \frac{B_{70} + B_{20}/2}{B_5} \times 100 \tag{1}$$

The value of diffusion factor has to be as near as possible to 100%. The total light transmittance and the diffusion factor can be controlled by changing the type and concentration of the light diffuser particles. [5]

Hiding power quantifies efficiency to mask hot spots. This value has to be as near as possible to 100%. [5]

$$H.P = \frac{T(2^\circ)}{T(0^\circ)} \tag{2}$$

Half angle value corresponds to the seeing angle, where light transmission drops down by 50 % in comparison to max light transmission. [5]

The table 2 lists optical properties of Milky materials made by company Altuglas.

Table 2: Typical optical properties of Milky materials [6]

Properties (2 mm thick samples)	**Diffuse 100**	**Diffuse 300**	**Diffuse 500**
Light transmission [%]	91	92	76
Relative Diffusing Power (1 inch)	25	53	67
Relative Diffusing Power (2 inch)	57	82	87
Hiding Power	0.98	0.99	0.99
Diffusion factor	0,16	0,28	0,34
Half angle value [°]	14	20	23,5

There are several factors in design of diffusers, which play a role in determining amount of diffusion. For example, thicker lenses - as well as those that have higher diffusion levels, have

better hiding power, however transmit less light. The distance between the light source and lens also play role into amount of light diffusion. The higher distance LED source from the diffuser, the higher diffusion effect. [4]

The figure 6 shows dependence of the thickness of the material PLEXIGLAS® LED white 0V606 on the luminance distribution. Luminance distribution is measured in material thickness 1, 2 and 3 mm and distance from the material to LED is 5 mm.

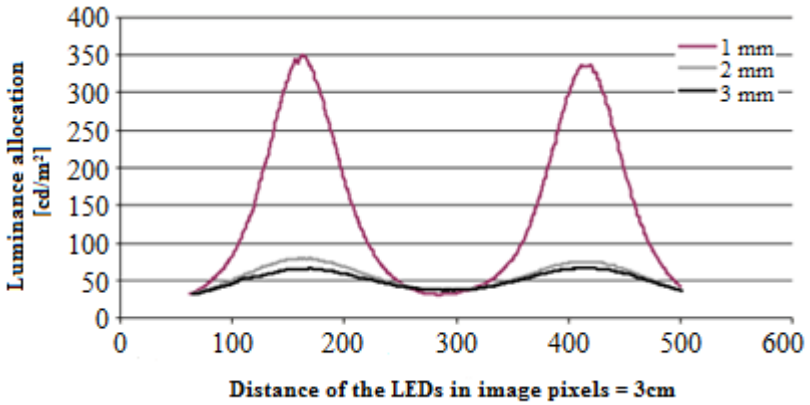

Figure 6: Dependence of the thickness of the material on luminance distribution [4]

Nowadays producers (Altuglas, Plexigals, Makrolon...) can offer various properties of this type of material with very good performance. The figure 7 shows 3 types of diffuse polymers made by company Altuglas. It is clear, that light transmittance decreases with increasing value of diffusing factor. Nevertheless, producers can offer very good ability of light transmittance (up to 91%). Due to surface losses, theoretical maximum transmittance is about 94%.

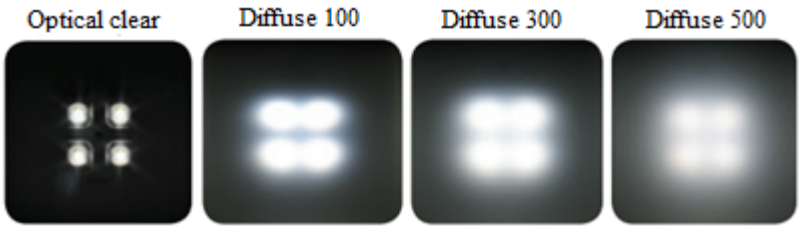

Figure 7: Types of diffuse polymers [6]

1.2 LED in automotive

LED lights have been produced for commercial lighting for a long time ago, however LED light sources for automotive lighting was first introduced in 2003 [7]. With the increasing LED technology and improving performance of LED lights sources, this technology has a potential gradually supplant commonly used light sources in automotive like incandescent light bulbs, fluorescent and halogen lights. In automotive lighting is usually used combination of several LEDs to create an interesting design-concept that creates a typical characteristic of a car.

Figure 8: Example of full led headlamp Volkswagen XLI designed by Varroc company [8]

Compared with all other types of automotive light sources, LED lights have some very distinct advantages, what make them perfect solution for automotive lighting. The main advantage of their using in vehicles is that produce more light per watt of energy (up to 100 lm/W) and they are capable radiate light in the required color without using color filters. The construction of LED is highly resistant to impacts and there is no a peak voltage during turn on and off. Low energy consumption is reflected on lower fuel consumption of vehicle, what leads to protection of environment and saving exhaustible energy resources. One of the advantages is longer lifespan, so it is not needed to change this source during lifespan of automobile. Additional advantage of LED is a start up to full light output (approximately 200 ms faster like standard bulb). This fact causes that response of driver on stop light is much faster, therefore can react faster. [9]

The main disadvantage of LEDs is their temperature dependence, which depends on the wavelength. With increasing temperature decreasing energy efficiency of LEDs, and thus an important luminous flux. This dependence is most evident in the yellow LEDs, while the least is evident in blue LEDs.

A light-emitting diode (LED) is semiconductor light source, which emits narrow spectral light when current passes through it in forward direction. This phenomenon is generally called electroluminescence, which is defined as the emission of light from a semi-conductor under the influence of an electric field. The wavelength of a radiated photon depends on its energy, so with higher energy, photon has less wavelength. The wavelength of emitted light can be influenced by

suitable dotation of semiconductors. For this dotation are used compound with elements from the first and fifth columns of periodic table.

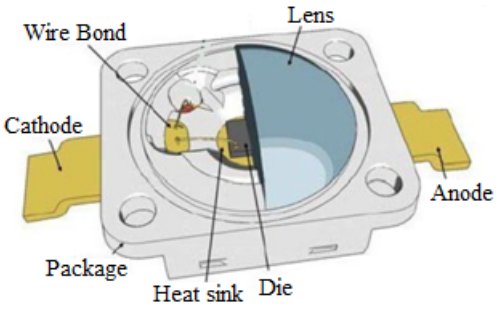

Figure 9: Constructin of single chip LED

The white light emitted by LED can be obtained by mixing of RGB colors or phosphorescence of phosphors. However, the second method is more often used in automotive lighting. This method uses yellow phospor coating known as YAG (Y3Al5O12:Ce), which is excited by blue InGaN diode. The phosphor coating absorbs a blue light and produces yellow light through fluorescence. The combination of yellow with remaining of blue light appears to the eye like a white. However, using different fluorescent materials it is also possible produce other colors. [9]

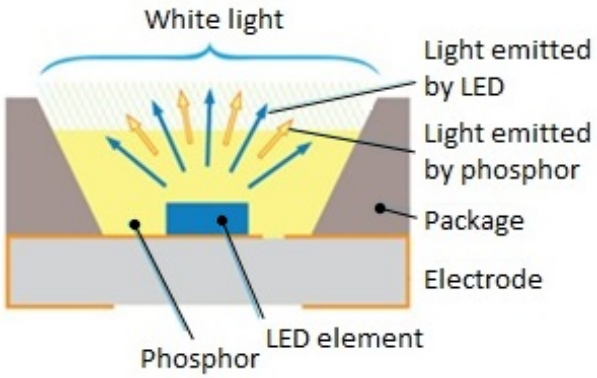

Figure 10: Principle of white LED

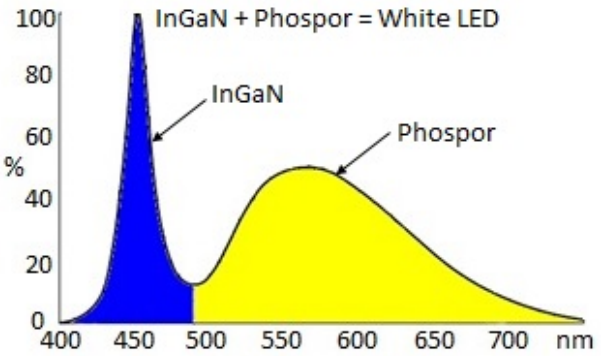

Figure 11: Spectrum of white LED

With the rapidly-developing lighting technologies and the introduction of new technologies, LED lighting manufacturers will produce even better comfort and homogenous light and more types of LED lights to meet a wide variety of vehicles. LED lights will have a bright future for automotive lighting application.

1.3 OLED in automotive

OLED technology is the next big step into the future of automotive lighting. Nowadays, LEDs technology have become standard for all car producers and prominent manufacturers have already begun to produce the first vehicles with OLED technology. OLED technology offers completely new possibilities in automotive lighting and luminaire design. It produces extremely homogeneous light surfaces in all shapes and plenty colors. Thanks to extensive research in recent years, OLED application in automotive lighting is durable and energy efficient. The most significant problem for organic light emitting diodes in automotive applications is thermal stability. To meet requirements of manufacturers, OLEDs in tail lights for example must resist temperature peaks of at least 85 degrees Celsius over several hundred hours as part of a long-term laboratory test. What is important, producers have worked towards solving this challenge with success. [10]

An organic light-emitting diode consists of several semiconducting organic layers sandwiched between two electrodes, at least one of them being transparent. The simplified device structure, which emits light to one-side is shown in figure 12. The device is fabricated by sequentially depositing organic layers on a conducting substrate followed by another conducting electrode. The organic stack including electrodes is usually thinner than 1 μm. Two types of organic materials are commonly used for OLED devices. The polymeric substances and "small molecule materials", which form amorphous films. When a DC bias is applied to electrodes, injected electrons and holes recombine in the organic layers and emit light of a certain color depending on the properties of the organic material. [10]

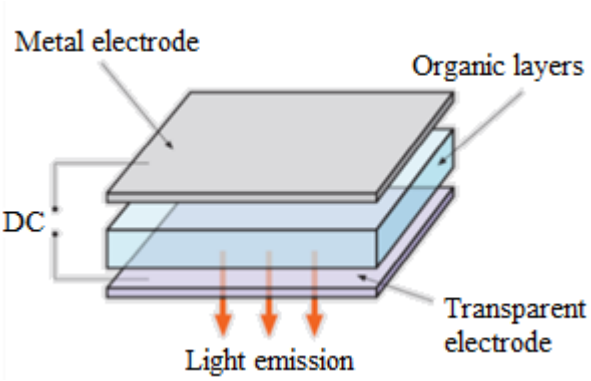

Figure 12: Principle of OLED technology

It is a new kind of luminous semiconductor and has almost no common feature with classical LEDs. OLED technology opens up new space in design options. Designer can create completely new luminous emblems in distinctive shapes and colors, features as transparency or flexibility are also on the horizon. One example of this future technology can be a third brake light integrated in the rear window.

In January 2015 manufacturer BMW demonstrated a new concept car, the M4 Concept Iconig Lights with two new lighting technologies - the laserlight headlights and the OLED based tail lights and rear direction indicators. The rearlights use yellow and red small thin OLED lighting panels made by Osram to create a 3D effect. During the car's unveiling, BMW said that they aim to launch a production model with OLEDs in the "near future". The picture bellow shows concept of rear lamps of this model. [11]

Figure 13: OLED rear lamp [11]

1.4 Laser light for headlights

Laser light is an absolute innovation in automotive lighting and the next big step forward since the introduction of LED and OLED technology. This modern lighting technology opens up entirely new space in the design and performance of headlights.

The main components of this technology are laser diodes, which generate extremely high luminosity in a very small space. This luminosity is far above the brightness of conventional technologies - four times more than LED technology. Due to extreme brightness, very small optical components can be used, thus creating a good deal of design freedom for the headlight designer. Extremely high intensity of light enables long range of light beam. However, using laser diodes in vehicles brings disadvantages, because they must function in a temperature window of - 40 to +100 °C what is one of the limitation aspects.

Car Makers BMW and Audi launched almost at the same time the first series production vehicles with laser headlights with models BMW i8 and Audi R8 LMX respectively. The laser module in the BMW i8 is integrated into the full LED headlights. They are activated when driving speed exceed 70 km/h and on-board camera can reliably see that on the road is no oncoming traffic.

The picture bellow shows the first experimental setup of BMW i8 headlight. Source of the light consists from three high-performance laser diodes, which emit coherent and monochromatic blue light with wavelength 450 nm. Laser beams are directed by using special lenses onto fluorescent phosphorous substance. This fluorescent substance converts beams into a white light

with a color temperature around 5500 K, which is very similar to daylight, however, still with a very high intensity. Subsequently, parabolic mirror reflects the white light with high intensity to the harmless dispersed light.

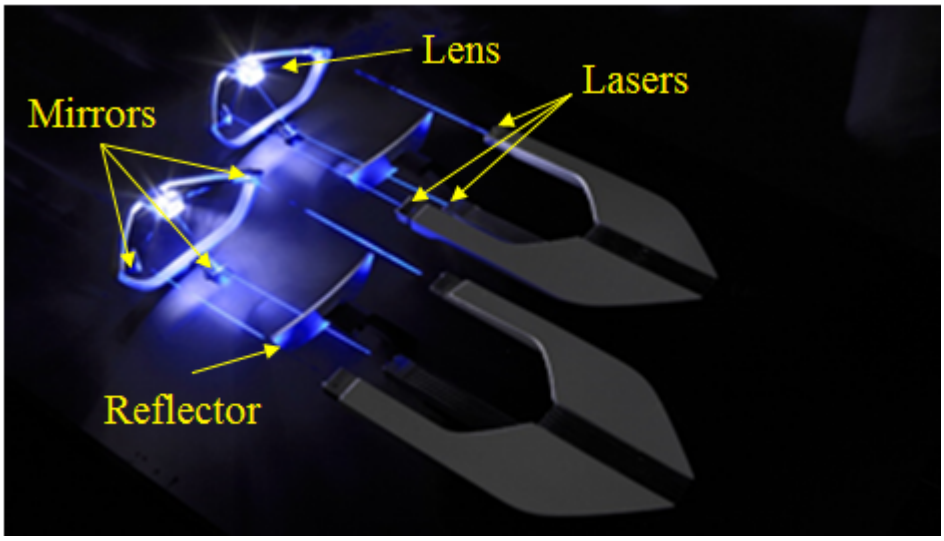

Figure 14: The experimental setup of BMW i8 laser headlight

These systems are still expensive solutions for premium vehicle manufacturer. However, the cost can be reduced by increasing volumes of production and this can be done by implementing laser headlights in mid-level vehicles. Laser diodes offer big potential for the future of the automotive lighting. [12]

2 Photometry in automotive lighting

Demands on light sources designed for the automotive industry usually vary considerably from the light sources used in the telecommunication industry and for illuminating of space. The light sources used in the automotive industry do not need fast response or high bandwidth. On the other side, these light sources place extra emphasis on a number of parameters and each has the same priority.

The human sight is not adapted to respond on effects of radiation over a period of time. For processes of vision is not important energy emitted over time, however the performance is crucial, therefore radiant flux especially spatial distribution. For this reason, energy values (e.g. radiant flux, radiance) are not considered in lighting technology, but it works with photometric quantities, which represent a different observer eye sensitivity to radiation of different wavelength. [13]

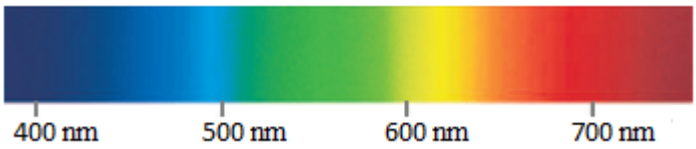

Figure 15: Visible spectrum of light

Photometry is measurement of visible light based on response of the average human observer. It is thus restricted to wavelength range from about 360 to 830 nm. Colours perceived by human eyes depends on wavelength. The amount of light energy detected by the eye at a particular wavelength determines the perceived intensity of that colour.

Radiometry is measurement of optical radiation, which is electromagnetic radiation within frequency range between 3×10^{11} and 3×10^{16} THz. This range corresponds to wavelengths between 0.01 and 1000 μm and includes region commonly called ultraviolet, visible and infrared [14]. The only real difference between radiometry and photometry is that radiometry includes entire optical radiation spectrum, while photometry is limited to visible spectrum as defined by response of the eye. The table 3 lists relationship between radiometric and photometric quantities.

Table 3: Photometric and Radiometric unit [15]

Radiometric Term	**Unit**	**Photometric Term**	**Unit**
Radiant flux	Watt	Luminous flux	Lumen
Radiant intensity	Watt/steradian	Luminous intensity	Candela
Radiance	Watt/steradian/m^2	Lumiance	cd/m^2
Irradiance	Watt/m^2	Illuminance	Lux

Thus, photometry is essential for evaluation of light sources and objects used for lighting, signalling, displays, and other applications in the automotive industry. Therefore, following

subsections are dedicated to important photometric quantities and the picture 16 illustrates relationship between them.

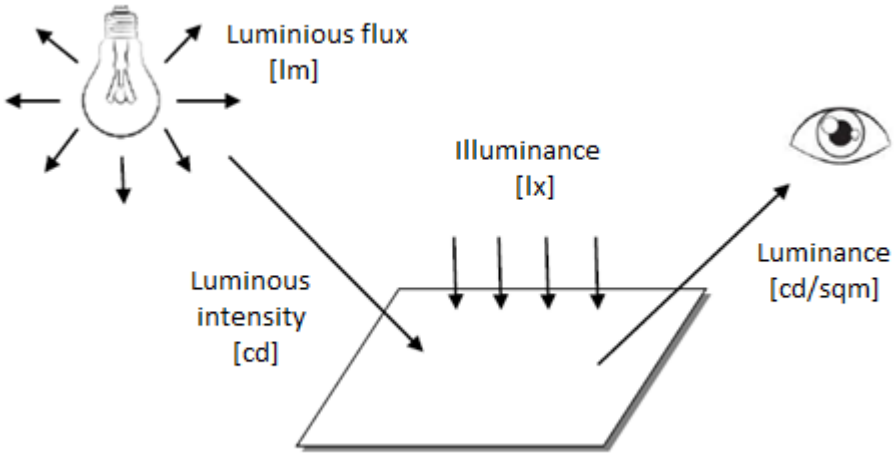

Figure 16: Relationship between photometric quantities

2.1 Basic photometric quantities

2.1.1 Luminious flux

Luminous flux is the quantity of energy of visible light radiated by a source. It differs from radiant flux, because luminous flux is adjusted to represent sensitivity of the human eye. The unit of luminous flux is the lumen (lm). Luminous flux Φ of monochromatic radiation with wavelength λ , whose radiant flux is Φ_e, is described by equations

$$\Phi(\lambda) = K(\lambda)\Phi_e(\lambda) = K_m V(\lambda)\Phi_e(\lambda) \tag{3}$$

$K(\lambda)$value is luminous effect of monochromatic radiation equals to the ratio of luminous flux and radiant flux. This value is often expressed by equation:

$$K(\lambda) = K_m V(\lambda) \tag{4}$$

Where K_m is the maximum value of a course of a function $K(\lambda)$ and $V(\lambda)$ is relative luminous efficiency. The relative luminous efficiency $V(\lambda)$ of monochromatic radiation is described by equation:

$$V(\lambda) = \frac{K(\lambda)}{K_m} \tag{5}$$

One lumen is defined as luminous flux of light produced by a light source, that emits one candela of luminous intensity over a solid angle of one steradian. [13]

2.1.2 Luminious Intensity

Luminous intensity is the luminous flux per unit solid angle emitted by a uniform point source of light. This is the quantity used to measure output of point (small) sources such as LEDs and miniature lamps. The SI unit of luminous intensity is candela (cd), and it is given in lumens per steradian: [13]

$$I = \frac{d\Phi}{d\Omega} \tag{6}$$

Scientific definition of candela is the luminous intensity, in a given direction of a source, which emits monochromatic radiation of frequency 540×10^{12} Hz and has radiant intensity in that direction of 1/683 W per steradian. This frequency corresponds to wavelength 555 nm. [14]

2.1.3 Illuminance

Illuminance or light level is the total luminous flux incident surface, per unit area. The unit of this quantity is lux (lx) or lumens per square meter ($cd\,sr\,m^2$). If $d\Phi$ is luminous flux and dA is area of the given surface then illuminance E is determined: [13]

$$E = \frac{d\Phi}{d\Omega} \tag{7}$$

One lx is illuminance of $1\,m^2$ surface area uniformly lighted by 1 lm of luminous flux. The drawing in the picture bellow explains this definition. Lux levels relevant to perception of light range from below 0.1 lux to above 120,000 lux. The lux value is used to describe amount of light in a given environment. [14]

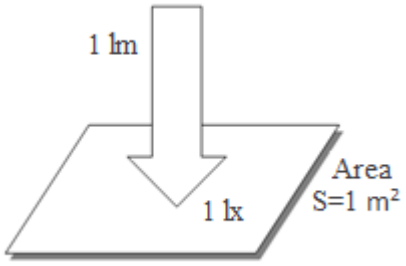

Figure 17: Graphic illutration of illuminance

2.1.4 Luminance

Luminance is the luminous flux emitted from a surface or extended source per unit solid angle per unit area in a given direction. Luminance is the only form of light we can see. Mathematically it is:

$$L = \frac{d^2\,\Phi}{d\,\Omega\,d\,A_n} \tag{8}$$

Where $d\,\Omega$is solid angle and $d\,A_n$is an area of the source surface perpendicular to given direction. The unit of Luminance is candela per square metre (cd/m^2) or nit. These two terms being interchangeable. The quantity 1 nit can be defined as a luminance of a purely white object being exposed to a light level of p lux. Luminance is the unit, which relates to the perceived brightness of a given object. Typical luminance values relevant to displays are between 100 and 10,000 nit. [13]

Due the reason, that light emitted from a surface can be created by reflection or direct emitting (e.g. LCD display), the relationship between luminous flux, illumination and luminance is not as simple as might appear. If the object is completely dark, then reflection factor is 0 and object is perceived as completely black no matter what the light level is. If the object is purely

white, reflecting all colours evenly in all directions, then reflection factor is 1. The standard reference material for reflection factor 1 is a surface of barium sulphate. This surface is also known as a Labertian surface. This kind of surface reflects light uniformly in a 180 ° hemisphere, no matter from which direction the light strikes it. [14]

2.2 Luminous efficacy

Luminous efficacy is a property of light sources, which indicates what portion of emitted electromagnetic radiation is usable for human vision. The effectiveness of illumination is defined by the ratio of luminous flux in lumen emitted by a specific source of light and the power in watts consumed by it. This power can be either total power (electric power) or radiant flux of the source. This fact is usually inferred from the context, however in our case it will be always electric power. The equation describes this light property is given

$$\eta = \frac{\Phi}{P} \tag{9}$$

where Φ is luminous flux and P is power consumed by light source. [13]

According to scotopic and photopic function (figure 22), theoretically attainable maximum value of luminous efficacy assuming complete conversion of energy at 555 nm would be 683 lm/W for photopic vision. Scotopic luminous efficacy reaches a maximum of 1700 lm/W for narrowband light of wavelength 507 nm. The luminous efficacies, that can actually be attained vary depending on the lamp. Electromagnetic power, which is useful for lighting is only a fraction of total power, which is emitted by the source. It is obtained by dividing luminous flux with radiant flux. Wavelengths near the peak of the eye's response contribute more strongly than those wavelengths, which are near the edges. Light with wavelengths outside visible spectrum does not contribute to the efficacy at all, because luminous flux of these wavelengths is zero. [14]

Table 4: Luminous efficacy of typical light sources used in automotive lighting [16]

Type	Luminous efficacy (lm/W)
Incandescent light bulbs	15 lm/W
Halogen lamps	30 lm/W
HID lamps	90 lm/W
LED	100 lm/W

The difference between efficacy and efficiency is that efficiency is expressed as a percentage. Maximum possible efficacy is 683 lm/W and it corresponds to an efficiency of 100%. The table 4 lists luminous efficacy of typical light sources used in automotive lighting.

3 Photometric measurement in automotive lighting

Photometric measurement in automotive lighting is realized in special dark room with using goniophotometer. Goniophotometer is a device used for measurement of the light emitted from an object at different angles. For measurement is used etalon source to guarantee repeatability. Etalon source defines standard ECE 37, as a source with nominal geometric and photometric properties [17]. Output of this kind of measurement is report about intensities of light in measuring points and isocandela map, that serve to validation of product. During the measurement of photometric quantities is necessary to avoid reflections. This is achieved by using anti reflective materials in the room.

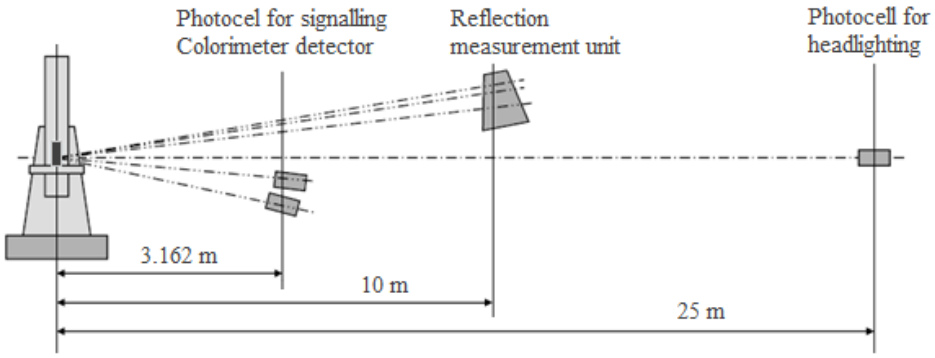

Figure 18: ECE photometry set

The picture 18 shows example of fully equipped ECE photometry set for automotive lighting. As apparent from the picture, photocell for headlights is located 25 metres from the goniophotometer on the wall together with measurement points. Typical placing of control points with minimal intensities shows picture 19. Other devices, photocell for signalling lights and colorimeter detector are located 3.162 m from goniophotometer. Retroreflector's measurement unit is located 10 metres from goniophotometer.

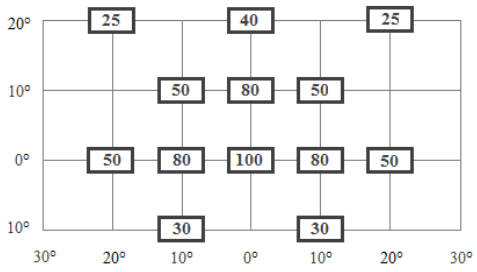

Figure 19: Typical distribution of control points

3.1 Measurement of luminance

With increasing demands on design of automotive lighting and usage of new light sources (LED) is also significant measurement of the luminance. Measurement of luminance, analysis of homogeneity of optical flux, is performed by digital camera with monochromatic chip along with the RGB filter. Due to wide dynamic range of luminance is a photo taken several times (minimum 12) at different times of exposure. Subsequently images are combined into luminance maps. Important thing is that the first picture is taken without any pre-saturated pixel. After that, captured images are transferred to the brightness. It is important that camera chip must be correctly calibrated. The digital camera takes constantly RGB values, which are converted to the model CIE (x, y, z). [16]

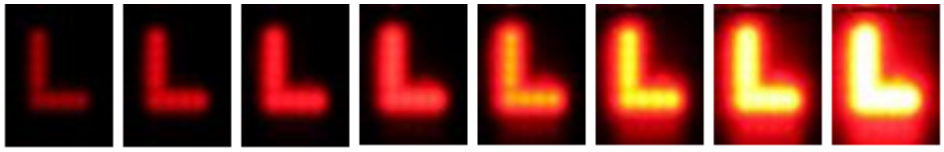

Figure 20: Photos of rear lamps with different times of exposure [16]

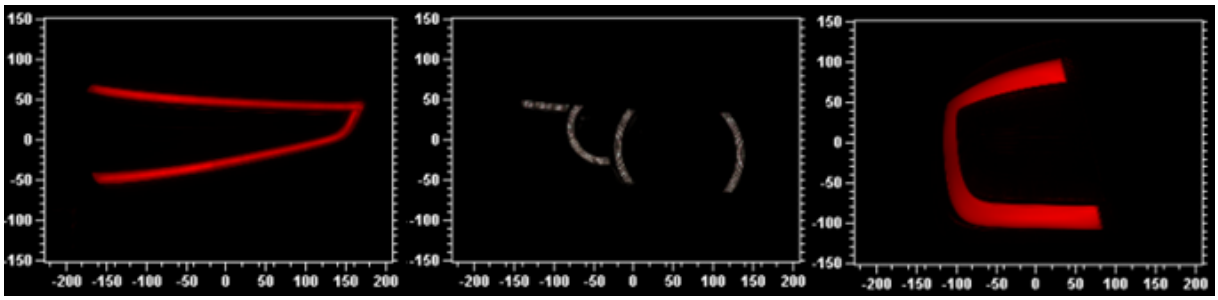

Figure 21: Luminance photos of lights [16]

4 Colorimetry

Colorimetry, the science of colour measurement is used to quantify and describe physically human colour perception. It is widely employed in commerce, industry and laboratory to express colour in numerical terms and to measure colour differences between specimens. The use and importance of colorimetry has grown gradually with the increase of global manufacturing and processing. When plastic automotive light produced on one continent, for example, must match with automotive light produced on another continent, an objective and precise description of colour becomes an absolute necessity.

The response of the eye to light depends on physical, physiological and psychological factors and varies from person to person. These factors make difficult to define average observer. The International Commission on Illumination (CIE) conducted a series of experiments in 1924 to quantify human eye response to visible light. After that, they created a specific spectral luminous function V (λ), which characterizes the daylight vision of average human observer. Due to response changes at low light levels, the CIE also defined a scotopic function V'(λ), which characterizes the response of the dark-adapted eye. [15]

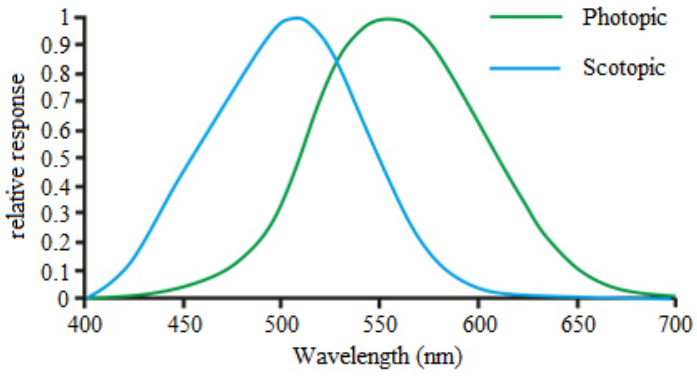

Figure 22: Photopic and scotopic function

Figure 22 shows the response at different wavelength for normalized photopic function and normalized scotopic function. Human eye is the most sensitive to green colour. Due this reason, spectral response is the greatest in green region, corresponding wavelength from 540 to 560 nm. Most people cannot see blue below 400 nm or red above 700 nm, so photopic response is almost zero in these regions. We can see the peak of scotopic response towards the blue region for two reasons. Colour receptors or cone cells of dark-adapted eye are off and monochromatic rod cells are primary sensors. The second reason is occurrence of rhodopsin (purplish liquid), that enhances night vision.

There are many color spaces for defining and mathematically expressing specific colour. However, the most widely used colour space in automotive industry is CIE's XYZ colour space established in 1931. This chromaticity diagram is shown in picture 23. The diagram is used for two-dimensional graphing of colour, independent of lightness. X and Y are chromaticicity

coordinates calculated from tristimulus values X-Y-Z. Achromatic colors are toward the center, and chromaticity increases toward the edges.

4.1 Colorimetry in automotive

Different colored signals in automotive have their own distinct meanings. Due to this reason, lighting functions have to be distinguished from each other according applicable rules. The colors of lighting functions and their definitions define regulation ECE 48. These colors are divided into three categories, while colors in each category are defined by the areas, which lie in the chromatic diagram (CIE xy). The table 5 lists required color of lighting functions and figure 23 shows chromatic diagram with specific boundaries for each color.

Table 5: Colors of automotive lighting functions

Color	**Function**
White	Lighting function
Amber	Turn indicators
Red	Position, Stop, Fog lamps, Reflectors

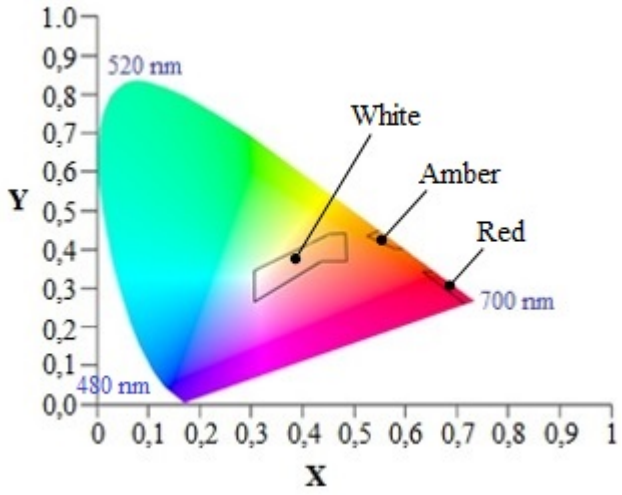

Figure 23: CIE xy chromatic diagram with specific boundaries for each color.

5 Optical principles used in automotive lighting

For automotive lighting application, dimensions of structures which the light interacts are much larger compared to the wavelength of light. Due to this reason, a description of behaviour of the light in automotive lighting is described by geometrical optics. Geometric optics, which might better be called ray optics, describe light propagation in terms of rays. The ray is the tool or an abstraction that is used to predict the path of light along, which light propagates it. This description neglects the wave character of the light and uses principle of rectilinear propagation of light, reciprocal independent propagation of rays, or refraction and reflection laws. These laws can be derived by using Fermat's principle. For an explanation of these principles is necessary to introduce basic value - refractive index.

5.1 Refractive index

Optical characteristics of material are completely specified by its refractive index. Refractive index of any material is a dimensionless number that describes how light propagates through the medium. This value, generally labelled with symbol n distinguishes two transparent optical media, that form interface. The index of refraction for any transparent optical medium is defined as the ratio of speed of light in a vacuum to speed of light in the medium, as given in equation:

$$n = \frac{c}{v} \tag{10}$$

where c represents the speed of light in free space (vacuum) and v is speed of the light in the medium. In a homogeneous medium is n same everywhere and in an inhomogeneous or heterogeneous medium index of refraction varies with position. The index also varies with the wavelength of light, cause dispersion and chromatic aberration in lenses. Index of refraction for free space is exactly one for air it is nearly one, so in the most calculation, it is taken to be 1.0. [18]

Table 6 lists indexes of refraction for common materials in automotive lighting.

Table 6: Refractive index for common materials in automotive lighting

Material	**Index of refraction**
Glass	1.5
PC	1.586
PMMA	1.492

5.2 Law of reflection and refraction

When a ray of light is incident of boundary separating two different optical media, part of the ray is reflect back into the first medium and the remainder is refract as it enters second medium. According to law of reflection, the angle of incident ray is exactly equal to the angle of reflected rays. The incident ray, reflected ray and normal always lie in the same plane. [19]

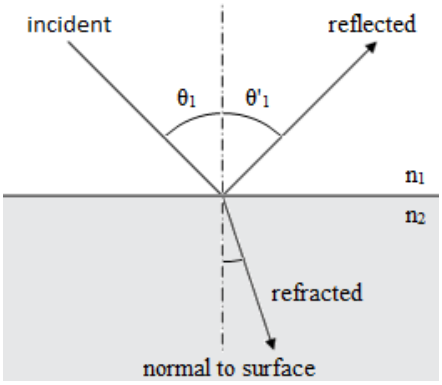

Figure 24: Law of reflection and refraction

Picture 25 shows two general cases, one for light passing from a medium with lower index of refraction to medium with higher index of refraction. Second figure shows the case, when light passing from a medium with higher index of refraction to medium with a lower index. In the first case (lower-to-higher), light ray is refracted towards the normal. In second case (higher-to-lower), the beam is bent away from normal.

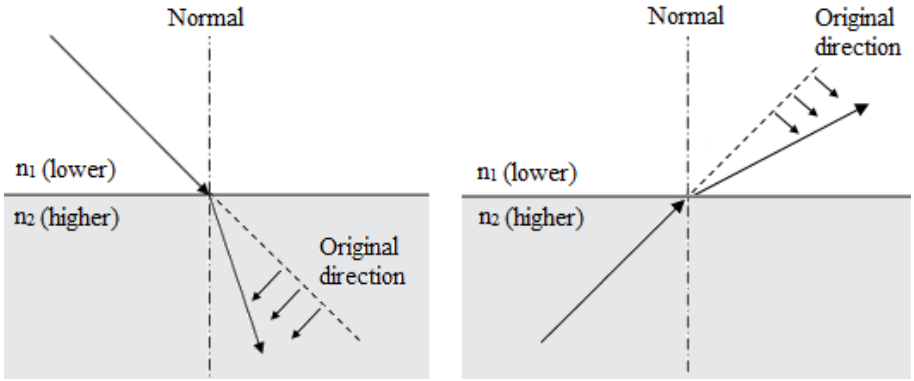

Figure 25: Light passing from higher and lower index of refraction

5.3 Snell's law

Snell's law gives the relationship between angles of incidence and refraction for a light impinging on an interface between two media with different indexes of refraction. The law is named after a Dutch astronomer, Willebrord Snell, who formulated law in the 17th century. Snell's law enables us to calculate the direction of refracted ray if we know refractive indexes of two media and direction of incident ray. [18] The equation of Snell's law is

$$sin\,\frac{\theta_1}{\theta_2} = \frac{n_2}{n_1} \tag{11}$$

where θ_1 is the angle of incidence, θ_2 is the angle of refraction,n_1 is the index of refraction of incident medium, n_2 is the index of refraction of refracting medium. In practice Snell's law is written as

$$n_1\,sin\,\theta_1 = n_2\,sin\,\theta_1 \tag{12}$$

5.4 Critical angle and total internal reflection

There are some interesting results when light travels from a medium with higher index of refraction to one with lower index. In the picture 26 are four rays of light originating from point 0 and each ray incident on interface at a different angle of incidence.

Ray 1 is incident on interface at 90° angle (normal incidence) so there is no refraction. Ray 2 is incident at angle θ_1 and refracts (bends away from the normal) at angle θ_2. Ray 3 is incident at the critical angle θ_c, and refracted ray is bent away from normal (N) in angle 90°, thereby travelling along the interface between two media. Ray 4 is incident on interface at an angle greater than critical angle, and is totally reflected in same medium from which it came. Ray 4 obeys the law of reflection, it means that the angle of reflection is exactly equal to the angle of incidence. [19]

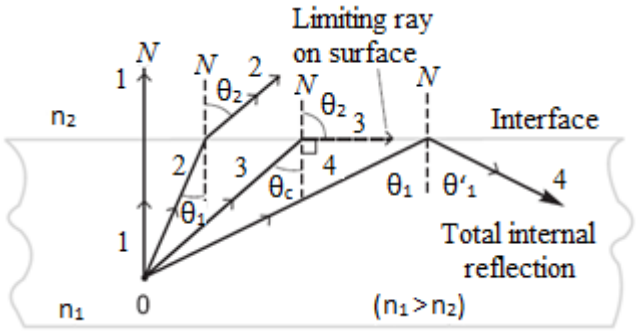

Figure 26: Critical angle and total internal reflection

The calculation of the critical angle of incidence for any two optical media, whenever light is incident from medium with higher index of refraction is given by the equation 13. The equation is based on Snell's law.

$$n_1 \, sin \, \theta_c = n_2 \, sin \, 90^\circ \tag{13}$$

where n_1 is index for the incident medium, θ_c is the critical angle of incidence, n_2 is the index for medium of lower index, and $\theta_c = 90\,^\circ$ is the angle of refraction at critical angle. Then, since $\sin 90\,^\circ = 1$, we obtain for critical angle following equation:

$$\theta_c = sin^{-1} \left(\frac{n_2}{n_1} \right) \tag{14}$$

Geometrical optics also helps understand use of simple optical elements used in automotive lighting such as mirrors, lenses and prisms. These matters are described in the following parts of this chapter. The figure 27 shows using basic optical principles in automotive lighting.

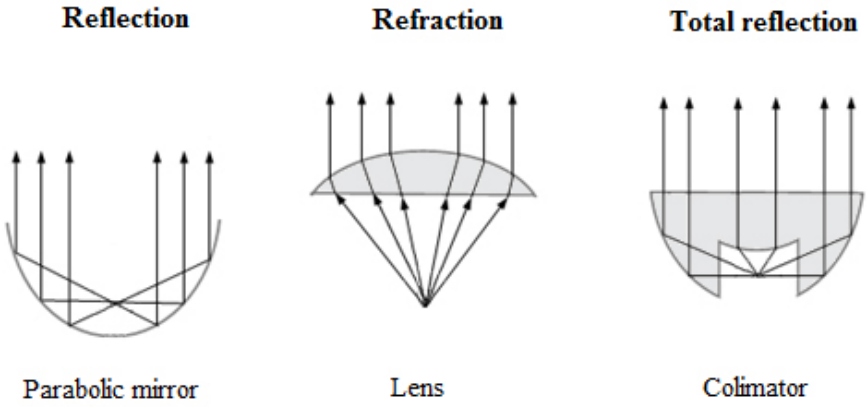

Figure 27: Optical principles in automotive lighting

5.5 Mirrors

Mirrors are objects, frequently used in automotive lighting. This subsection describe the basic principles of plane mirror and two special types of mirrors, parabolic and elliptic, which are often used for design automotive lights.

Quality of material of mirror impacts on efficiency of light source, as well as on spectral composition of reflected light. Nowadays, mirrors (reflectors) used in automotive lighting are made from low cost plastic, which is covered by a thin layer of reflective material. The table 8 lists reflectance of various surfaces.

Fundamental principle of the flat mirror is that reflects rays coming from a point O (Object) so, that reflected rays appear like coming out from point I (Image). This point lies behind the

Table 7: Reflectance of various surfaces [16]

Surface	**Reflectance**
Magnesium Oxide	95%
Aluminum metallized reflector	85%
Polished aluminum	60%-80%
Road surface (light):	20%-30%
Road surface (dark):	5%-15%

mirror and is called an object. The distance of subject O from the mirror is identical to the distance of image I from mirror. [19]

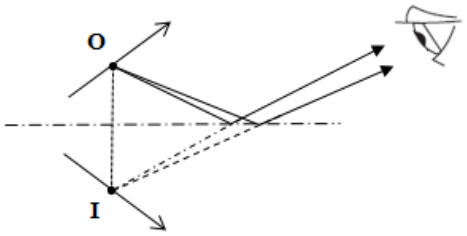

Figure 28: Principle of flat mirror

Parabolic mirror

The shape of parabolic mirror is part of a circular paraboloid that means the surface of parabola rotates around its axis. Parabolic mirror collects rays, which pass through focal point, and reflects their parallel to optical axis. In the case that light source is located before focal point, convergent beam is created. If light source is shifted behind focal point, reflected beam diverges. [20] In automotive lighting is this basic shape of mirror used in headlamp and rear lamp design. The principle of this kind of reflector and its practical using in automotive is shown in figure 29.

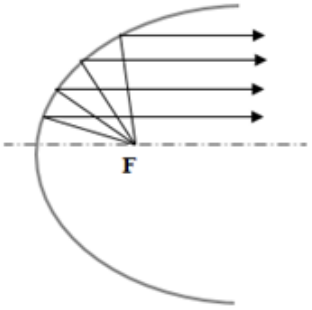

Figure 29: Parabolic mirror

Elliptic mirror

Elliptic mirror in opposite to parabolic mirror has two focal points, which always lie on major axis. Every light ray which passing through first focal point, is reflected in second focal point. A shift of the light source before or behind the focus is manifested by changing direction of reflected rays. Due to the fact, that light source has always certain dimension, light rays reflected from every point are slightly divergent and do not pass precisely through the second focal point. With reduction of dimension of light source and increasing size of reflector, consequent rays are situated more accurate in focal point [20]. This mirror is used in projector design of headlamp as it is shown in figure 30.

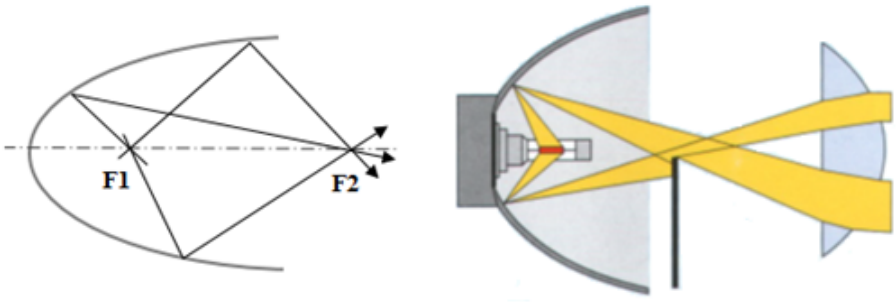

Figure 30: Elliptic mirror

5.6 Lenses

Lenses are light-controlling elements, used primarily for image formation with light. They have surfaces, which are spherical shaped on the front and back and are made up from a transparent refracting medium, typically from some type of glass. Snell's law determines the imaging properties of lenses. A ray incident on lens refracts at the front surface, passes through lens and refract again at the rear surface [20]. Figure 31 shows basic principle of lens. Thick lens refracting rays from an object OP to the image O'P'.

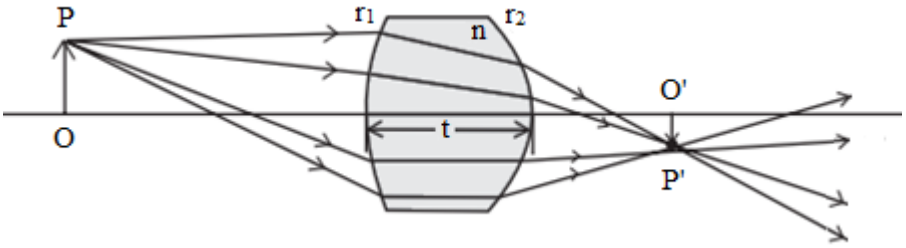

Figure 31: Principle of lens

Type of lenses

The figure 32 shows several common shapes of thin lenses. The first three lenses are described as convergent or positive lenses. They are converging because parallel rays passing through lens converges to a focal point behind lens. These types of lenses give rise to positive focal lengths. The last three lenses are described as diverging or negative lenses. In contrast with converging lenses, they cause parallel rays passing through them to spread as they leave the lens. Such lenses have negative focal lengths.

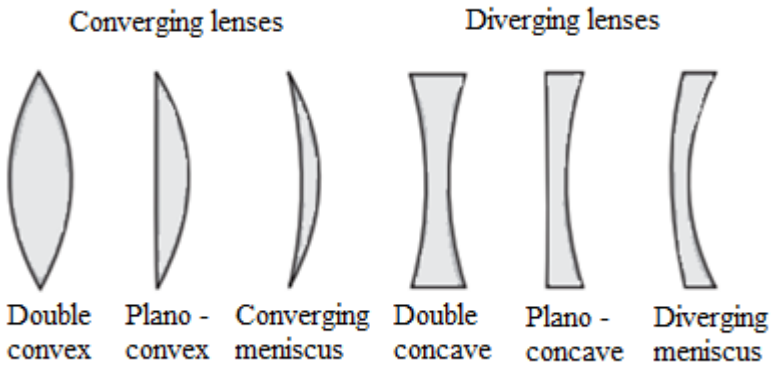

Figure 32: Type of lenses

A lens is biconvex if both surfaces are convex. A lens with two concave surfaces is biconcave. If one of the surface is flat, the lens is plano-convex or plano-concave depending on the curvature of other surface. A lens with one convex and one concave side is convex-concave or meniscus.

There are two focal points for thin lenses, which are symmetrically located on each side of lens, since light can approach from either side of lens. The picture 33 indicates the role of focal points for positive lenses (figure a) and negative lenses (figure b).

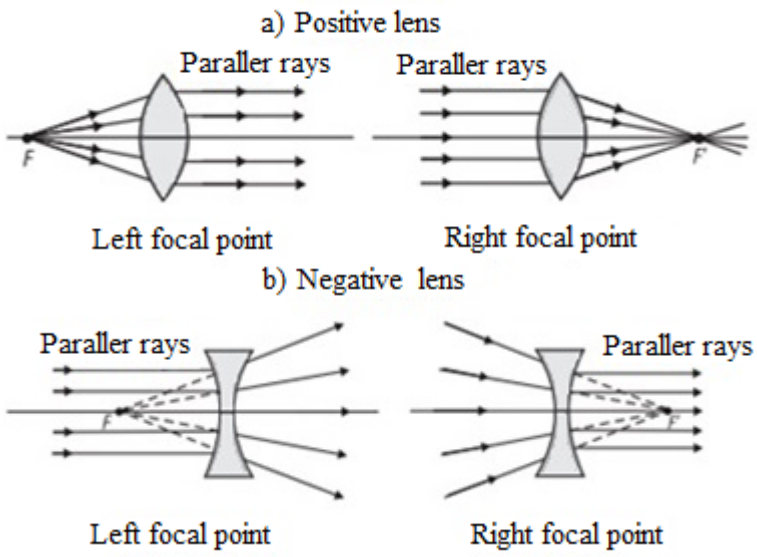

Figure 33: Focal points of a) positive lenses and b) negative lenses

The focal length of thin lens can be calculated by thin lens formula

$$\frac{1}{p} + \frac{1}{q} = \frac{1}{f} \tag{15}$$

where p is the object distance and q is the image distance.

For a lens of refractive index n_g situated in a medium of refractive index n, the relationship between the parameters n, n_g, r_1, r_2 and the focal length f is given by the Lensmaker's equation in equation

$$\frac{1}{f} = \left(\frac{n_g - n}{n}\right)\left(\frac{1}{r_1} - \frac{1}{r_2}\right) \tag{16}$$

where n_g is the index of refraction of lens materials, n is the index of refraction of surrounding medium, r_1 is the radius of curvature of the front face of the lens, r_2 is the radius of curvature of the rear face of lens. [20]

Fresnel lens

Lenses in automotive lighting have to have small focal length. It means, that they are strongly convex and therefore very thick. Due to these facts, for applications in automotive lighting are sometimes used Fresnel lenses. The Fresnel lens is a special type of lens that replace curved surface of a conventional optical lens with a series of concentric grooves. The grooves act as individual refracting surfaces, like tiny prisms, which bends parallel rays to a very close focal length. The sketch and principle of this lens are shown in the picture 34.

Refracting surfaces of conventional lens remain, while the rest of the bulk is reduced to a flat piece of equal thickness. A Fresnel lens is therefore much thinner than a normal lens, what brings

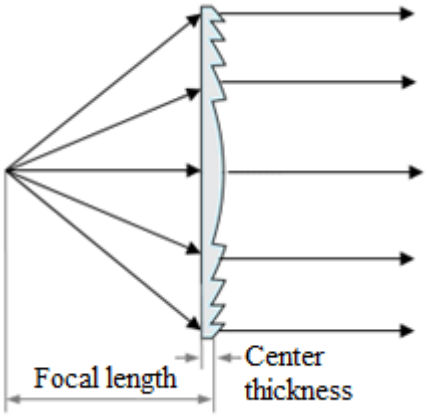

Figure 34: Fressnel lens

advantages like saving place or the fact that very small part of the light is lost by absorption. The next advantage of Fresnel lens is that the prism in the outer region can be used as reflection teeth. The light is then reflected at the outer surface via total internal reflection, therefore lens can combine both refraction and reflection.

Fresnel lenses are a compromise between efficiency and image quality. High groove density allows higher quality images, while low groove density yields better efficiency. Using of this kind of lens in automotive lighting is very hard. However, it is used for third rear lamp sometimes.

Figure 35: Fressnel lenses like third stop lamp [16]

5.7 Prism

Prism is transparent optical element with flat, polished surfaces that refract light. The process of refraction in prisms is understood easily with the use of light rays and Snell's law. When a light ray enters a prism at one face and exits at another, the exiting ray is deviated from its original direction. It is afocal element; it means that parallel beams after passing through prism are parallel again. Prisms are made in many different shapes, but the basic type of prism is triangular. The picture 36 shows prism, which is isosceles with apex angle A=30 ° and refractive index n = 1.50.

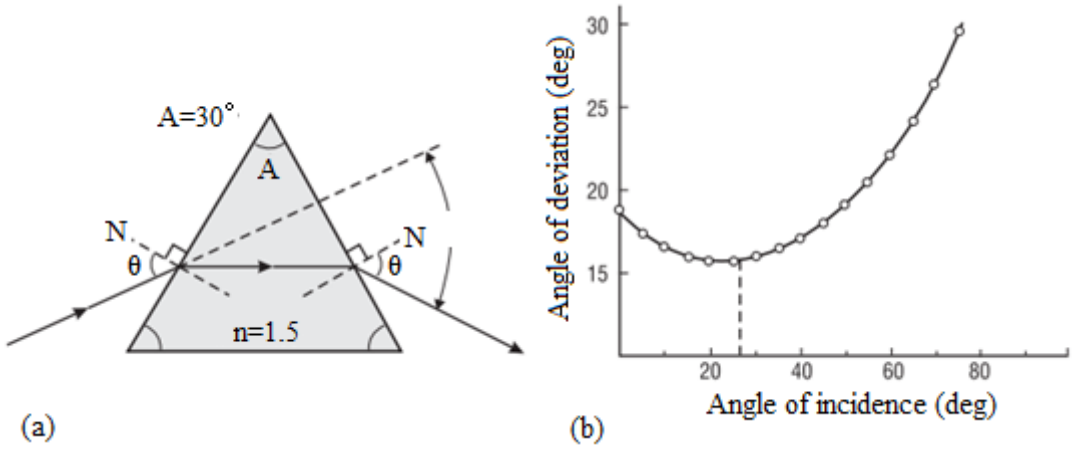

Figure 36: a) Principle of prism, b) Relationship between angle of devation and the angle of incident ray

Each prism material has its own unique minimum angle of deviation. The relationship between angle of deviation δ and the angle of the incident ray θ for our specific prism is in the picture . The deviation angle of thin prism varies with wavelength according to

$$\delta(\lambda) \approx [n(\lambda) - 1]\,\alpha \tag{17}$$

A standard triangular prism can separate white light into its constituent colours, called a spectrum. Each wavelength of entering beam is bent or refracted in different angles. Shorter wavelengths are bent the most and longer wavelengths are bend the least. This effect is called dispersion and is caused by fact that index of refraction depends on wavelength. [19]

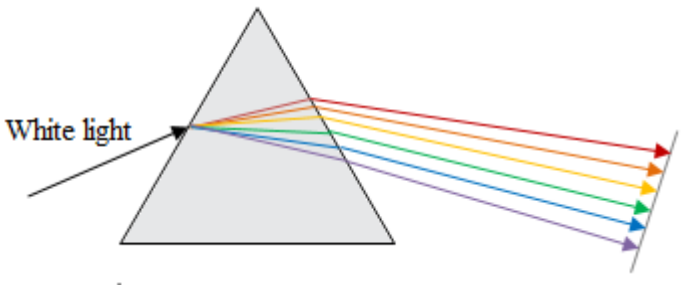

Figure 37: Dispersion of light caused by prism

5.8 Collimator

Collimator is optical element based on parabolic reflectors. It focuses light from focal point and change the direction of propagation rays to parallel rays. The light rays from a source, that are usually located behind collimator, are always spread to same direction.

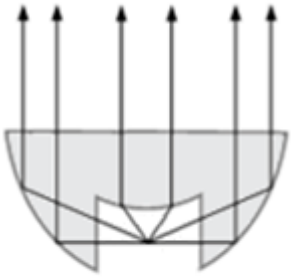

Figure 38: Collimator

From the picture 38 is clear, that light beams propagate in any direction from a source, are reflected from the collimator always under desired angle. The picture shows ideal collimator, focus of light to desired point or to desired angle can be avoided by changing inclination of the side.

5.9 Light-technical properties of materials

Optical properties of material are significant for design and construction of the light active parts of devices. Considering the luminous flux orientations, its diffusion and optionally brightness limitations in some directions. While, the highest possible efficiency is preserved. Luminous flux incident on considered material is in general case divided into three parts. Part, which is reflected, part that passes through the material and part of luminous flux, which is absorbed by the material. The following table lists these factors.

Table 8: Integral factors of luminous flux [13]

Integral factor of reflectance	$\rho = \Phi_\rho/\Phi$
Integral factor of transmittance	$\tau = \Phi_\tau/\Phi$
Integral factor of absorption	$\alpha = \Phi_\alpha/\Phi$

These quantities characterize the properties of observed materials from the view of different wavelengths collectively - integrally. For factors ρ, τ, α is applied known relationship

$$\rho + \tau + \alpha = 1 \tag{18}$$

For transparent materials is applied $\rho + \tau = 1$, and for materials that absorb all the light that falls on it, is applied $\alpha = 1$. Factors of reflectance, transmittance and absorption depends not only on properties of material, however also on wavelength of incident light. Due to this fact, for these factors are defined their spectral values $\rho(\mathrm{y})$, $\tau(\mathrm{y})$, $\alpha(\mathrm{y})$. [13]

6 Volume scattering

Electromagnetic waves impinging on material induces oscillating charges, which can be further radiated as secondary sources of radiation. The microscopic structure of explored material determine the properties (frequency, intensity, polarization...) of scattered radiation. The application of light scattering constitutes the basis characterization tool in biology, colloid chemistry and so on, in long history. However, with the gradual using of new progressive material in automotive lighting such as Milky material of PMMA or PC, is important to deal with this issue in this thesis thoroughly. Due to reason, that Milky material contains tiny particles, body of this application deals with light scattering by particles. The light scattering by single particles forms block of more complex physical situations. Volume scattering is classified like the physical process of wave interaction with matter, when the three dimensional size of the medium, which scatters the light is much larger than the typical size of a local inhomogeneity. The measured light originates from many separate locations distributed throughout the volume. Due to different structural characteristics of the medium, scattering centers can act as secondary independent sources of radiation (incoherent scattering) or they can partially add their contribution in a collective matter (coherent scattering). Interesting situation occurs for highly disordered systems (Milky material) when light is scattered successively at many locations throughout the volume of material. This situation is known as multiple scattering.

In practice, particles very rarely exist single, thus scattering by a large number of particles needs to be considered. The simplest case is incoherent scattering. In case, the fields scattered by different centers are entirely independent, the measured intensity is sum of all individual contribution of these intensities. The collection of particles is described by temporal and spatial statistics. However, spatial distribution of particles does not show up in experiments, so one can say, that volume scattering does not resolve the spatial distribution of scattering centers.

In case, the scattering centers are sufficiently close, the phases of scattered waves originating from individual scattering centers are addicted. This is situation of collective or coherent scattering. In this case, must be considered, that ensembles of particles can have certain degree of spatial or temporal correlations. The situation is common for gels or composites which scatter light due to local inhomogeneities of the refractive index. The coherent scattering is basis of successful application of volume scattering: observation of structural characteristic of inhomogeneous systems.

When the systems are highly disordered, the light propagation can be scattered at many different locations within the explored medium. It means, that multiple scattering regime sets in. The fluctuation of intensity and phase determined by multiple light scattering can be regarded as optical noise that degrades radiation by altering its coherence, broadenin the beam, and decreasing its intensity. However, in case using this phenomena in materials such as Milky PMMA or PC, can be achieved high homogeneity of light. Due to reason, that multiple scattering is basis of volumme scattering in Milky material, it will be described in specific chapter. [18]

6.1 General theory of scattering

The picture 39 shows the scheme of typical scattering incident. A plane wave $\mathbf{E^0}$ with the wave vector $k = \omega/c$ impacts on a spatially random medium with a finite volume V. Light is scattered by local inhomogeneities with the dielectric constant $\varepsilon(\mathbf{r})$. The basic theory of scattering is providing connection among intensity $I_s(\mathbf{R}) = |\mathbf{E_s}(\mathbf{R})|^2$ and the microscopic structure of the random medium.

For describing of this theory, is needed firstly describe the total electric field $\mathbf{E(r)}$ as a summation of the impacting and scattered fields. Consequently, it is necessary to consider that it satisfies the equation

(19)

where $\mathbf{S(r)}$ represents a generic scattering potential.

This formula can be transferred into an integral one, for $\mathbf{R}$ sufficiently far from the scattering volume. General result can be obtained by associating simplification Green function.

$$\mathbf{E}_s(\mathbf{R}) = \frac{e^{ikR}}{R}\frac{k^2}{4\pi}\int_{(V)} d\mathbf{r}\left\{-\mathbf{k}_s \times [\mathbf{k}_s \times (\varepsilon(\mathbf{r}) - 1)\cdot \mathbf{E}(\mathbf{r})]\right\} e^{-i\mathbf{k}_s\cdot\boldsymbol{r}} \tag{20}$$

This equation introduce the scattered field as an outgoing spherical wave, which depends on direction and magnitude of the total field within the scattering volume V.

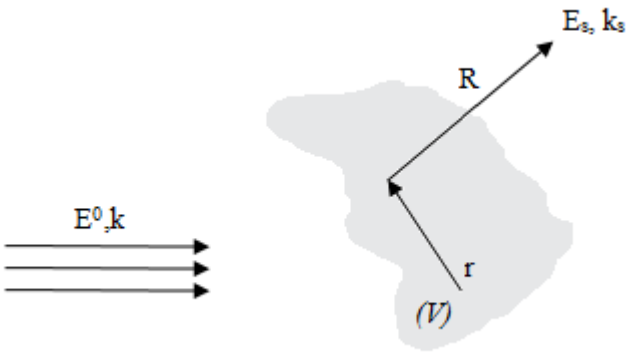

Figure 39: Schematic representation of the incident and scattered beams in a generic scattering experiment

In the case of weak fluctuations of the dielectric consant, approximate solutions can be obtained. The field $\mathbf{E}(\mathbf{r}) = \mathbf{E}^0(\mathbf{r}) + \mathbf{E}_1(\mathbf{r}) + \mathbf{E}_2(\mathbf{r}) + ...$ can be expanded in terms of increasing orders of the scattering potential and using successive approximations of $\mathbf{E(r)}$ in equation 20 are obtained Born series. Under the first iteration, where $\mathbf{E(r)}$ is replaced by $\mathbf{E}^0(\mathbf{r})$ the first Born approximation is obtained. This approximation describes the regime of single scattering. Alternatively, the series solution for $\mathbf{\Psi}(\mathbf{r})$ can be developed by rewriting $\mathbf{E}(\mathbf{r}) = exp\,[\mathbf{\Psi}(\mathbf{r})]$ in

terms of increasing orders of the scattering potential. This is the Rytov's series of exponential approximations, an alternative to the algebraic series representation of the Born method. These approximation are almost equivalent, however Rytov's method is preferred sometimes, because an exponential representation is more appropriate for describing waves in line-of-sight propagation problems.

It should be pointed, that equation can be considered as an integral equation for the total field. However the total field is a superposition of the incident field and contributions originating scattering from all volume V, this equation includes all possible multiple scattering effects. [18]

6.2 Multiple scattering

In case, when optical waves propagate through media with random distribution of the local inhomogeneites, or when waves encounter to extended regions containing discrete scatterers, it is necessary to solve a wave equation in the participation of huge number of scattering centers. For this task have been proposed a series of simplifying approaches, which will be described in this chapter.

Some physical concept is given by an elementary model that defines attenuation of the wave due scattering and absorption in terms of an effective dielectric constant. Without entirely involving of multiple scattering, it assumes, that the wave propagates through a homogeneous effective-medium, which is defined in terms of average of quantities. The effective permittivity ε_{eff} is calculated by considering the medium as a distribution of spherical particles with permittivity ε distributed in a continuous medium of permittivity ε_0. In case, when wavelength of a wave is much larger than the characteristic length scales (size of inhomogeneity and mean separation distance), and wave propagates through a volume random medium, the attenuation due to scattering can be neglected. Based on an induced dipoles model, the Maxwell-Garnett mixing formula relates the effective permittivity to the volume fraction v of spheres

$$\varepsilon_{eff} = \frac{\varepsilon(1 + 2va)}{(1 - va)} \tag{21}$$

where

$$a = \frac{(\varepsilon - \varepsilon_0)}{(\varepsilon + 2\varepsilon_0)} \tag{22}$$

The wave propagation through highly scattering media can be described by including multiple scattering interactions in a mean-field approach. This is simply done by considering that the energy density is uniform. A coherent beam is propagated through this effective medium with a propagation constant that includes the attenuation due to absorption and scattering. Generally, the propagation of the coherent beam is defined by a complex index of refraction associated with the effective medium. Thus, a nontrivial dispersion law can be determined by resonant scattering. It should be pointed, that for waves with longer wavelength, the attenuation due

to scattering is negligible, thus the classical mixture formula for the effective permittivity is applied. [18]

6.3 Analytical theory of Multiple scattering

In case, when statistical considerations are introduced for quantities such as variances and correlation functions for $\varepsilon(\mathbf{r})$, strict description of multiple light-scattering phenomena can be made. Subsequently, general wave equation are produced. This analytical theory has the advantage that the general formulation does not require a priori assumptions about the strength of individual scattering event. The packing fraction of scattering centers are not required as well. There is also a drawback, because in order to deal with the complexity of the problem, it is needed use approximations and formal representation.

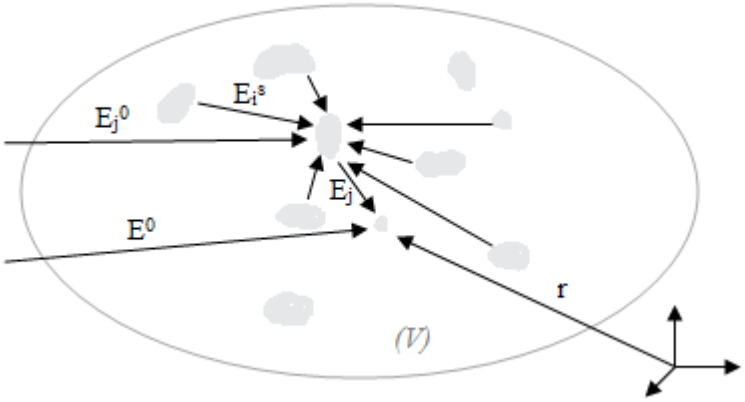

Figure 40: The field at $\mathbf{r}$ is a summation of the incident field $\mathbf{E}^0$ and contributions $\mathbf{E}_j$ from all other scattering centers; in turn, the effective field on each particle consists of an incident contribution $\mathbf{E}_j^0$ and contributions $\mathbf{E}_i^s$ from all other scattering centers.

The figure shows field $\mathbf{E}^0$ impacts on a random distribution of N scattering centers located at $\mathbf{r}_1, \mathbf{r}_2, ..., \mathbf{r}_N$ throughout the scattering volume V. The total field at one specific location inside volume V is the summation of the incident wave and the contributions from all the other particles. The total field at one specific location inside volume V is the summation of the incident wave and the contributions from all the other particles.

$$\mathbf{E} = \mathbf{E}^0 + \sum_{j=1}^{N} \mathbf{E}_j \tag{23}$$

the field scattered from the jth particle depends on the effective field incident on this particle and its scattering potential S_j

$$\mathbf{E}_j = \mathbf{S}_j(\mathbf{E}_j^0 + \sum_{i=1, i\neq j}^{N} \mathbf{E}_i^s) \tag{24}$$

From equations 23 and 24 results, that the total field can be formally written as

$$\mathbf{E} = \mathbf{E}^0 + \sum_{j=1}^{N} S_j(\mathbf{E}_j^0 \sum_{j=1}^{N} \sum_{i=1, i\neq j}^{N} S_i \mathbf{E}_i^s) \tag{25}$$

This equation consists of single scattering series, increasing orders of multiple scattering and series of contributions from the incident field. If it is known scattering characteristics (strength and location) S_j of individual centers, analytical approach can be developed by involving chains of successive scattering paths. From the summations in equation 25 and neglecting the scattering contributions that contain a scatterer more than once, can be developed an expanded representation of multiple scattering. However, it is practical only for cases of low-order scattering. This representation was developed by Twersky. [18]

7 Simulations of optical elements from Milky material

In the theoretical part of this thesis was explained basic physical phenomena and properties of Milky materials. This chapter describes process of simulation of various optical elements made from Milky and transparent materials as well as their comparison. The first subsection describes used geometry where were tested optical elements. Subsequent parts concern with simulations of the individual optical elements. Tested geometry and individual optical elements were designed in CAD software Catia. Optical properties of these elements were subsequently simulated in the 3D optical software LighTools. For evaluating results from simulations and creating iso candela maps was used software BeamAnalyzer. Lit appearances of final simulation were rendered in program Blender and LuxRender. The entire practical part of this thesis was done in Varroc Lighting Systems.

7.1 Description of measurement

As I have mentioned above, simulated geometry was designed in software Catia. This geometry represents rear position lamp situated on right side of the car. Rear position lamp means the lamp used to indicate the presence and the width of the vehicle when viewed from the rear [21]. Tested geometry – rear position lamp is shown in figure 41.

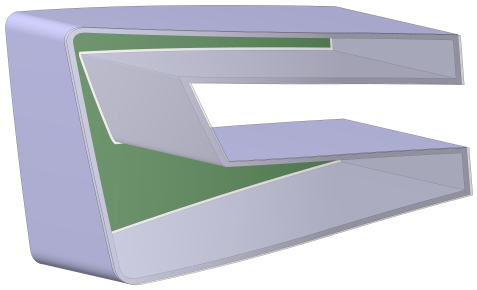

Figure 41: Simulated geometry: rear-right position lamp

Tested geometry consists of three main components (figure 42). First component is printed circuit board (PCB) where are mounted 28 LEDs. LEDs OSRAM-LA T67F were used as the light sources (each LED emits 1 lm). Datasheet of this LED is included in Annex A. Next component is a tube of mirror with 80% of reflectance. The last and the most important component for simulations is Milky filter where will be placed tested optical elements. Milky filter was changed for transparent material in final simulations, due to comparison of optical differences among them.

The figure 43 shows regulation ECE 7 for rear position lamp with zones of lighting. As shows this picture, visibility of rear position lamp shall be vertically $\pm 15\,^{\circ}$, horizontally $45\,^{\circ}$ inside, and $80\,^{\circ}$ outside, respectively. The light emitted by rear position lamps shall be in the reference axis of not less than the minimum intensity (4 cd) and of not more than the maximum intensity (17

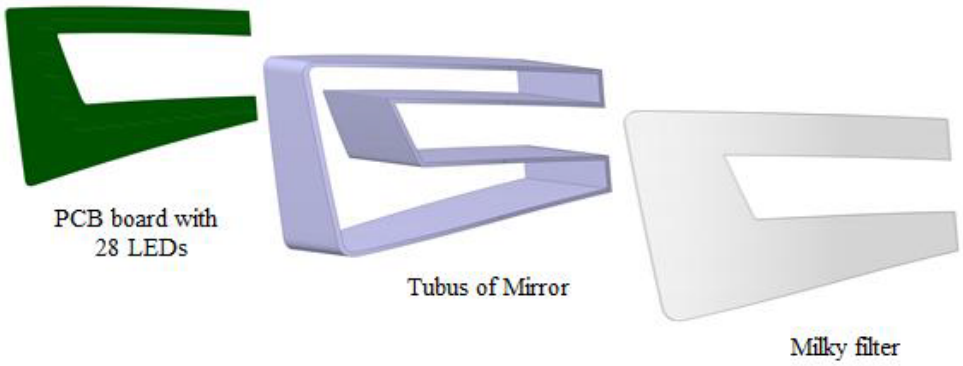

Figure 42: Individual part of simulated geometry

cd). The direction H = 0 ° and V = 0 ° corresponds to the reference axis. On the vehicle, it is horizontal, parallel to the median longitudinal plane of the vehicle and oriented in the required direction of visibility. It passes through the center of reference. [21]

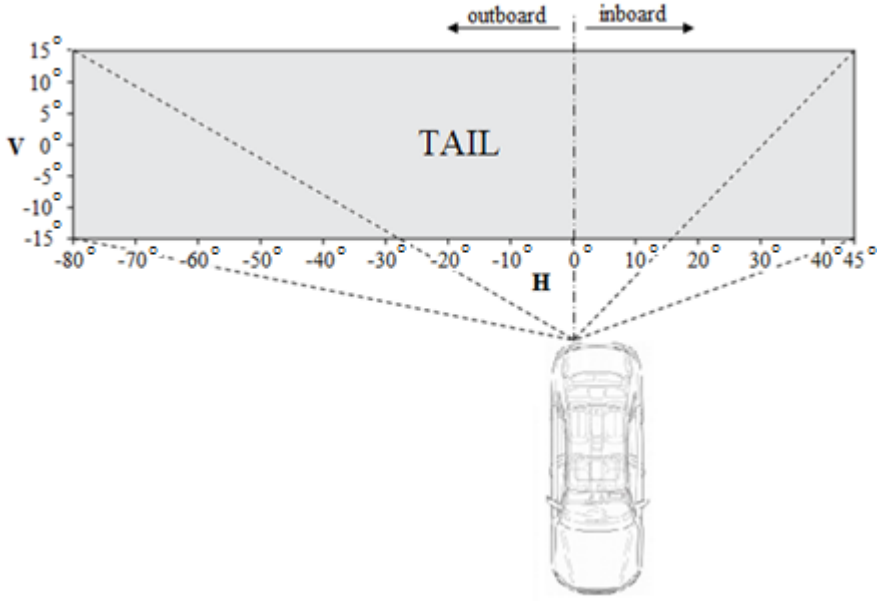

Figure 43: ECE 7 regulation for rear position lamp

The figure 44 shows iso candela map of simulated rear lamp with values of luminous intensity in measurement points. As it is clear from the iso candela map, values on the left side of the map (visibility on -80 °) do not meet standard ECE 7 for rear tail-right lamp. These values are displayed in the table with red color. The aim of following simulations in this chapter will meet the standard by using of different optical elements placed on the Milky filter.

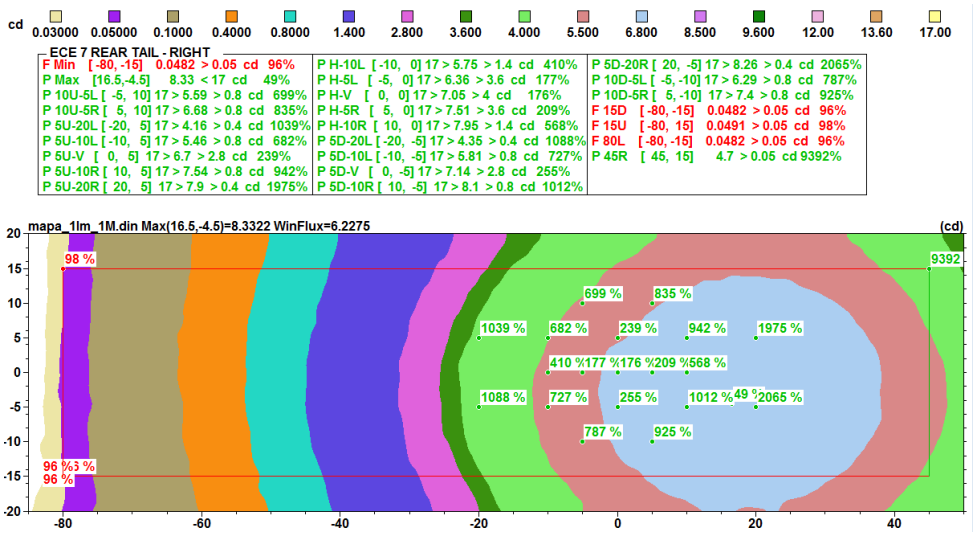

Figure 44: Iso candela map of simulated geometry

Lit appearances are used to evaluate the homogeneity of the emitted light in false colours. However, for a better evaluation of homogeneity are final simulations created in software LuxRender. The following figures show lit appearances of simulated rear lamp. In the figure 45 is lit appearance created in LightTools software, the figure 46 shows lit appearance of geometry with Milky filter created in LuxRender. The figure 47 shows lit appearance of origin-simulated geometry but with transparent filter. Due to the saving of processing power was lit appearance created in LuxRender just for final simulations of the individual optical elements.

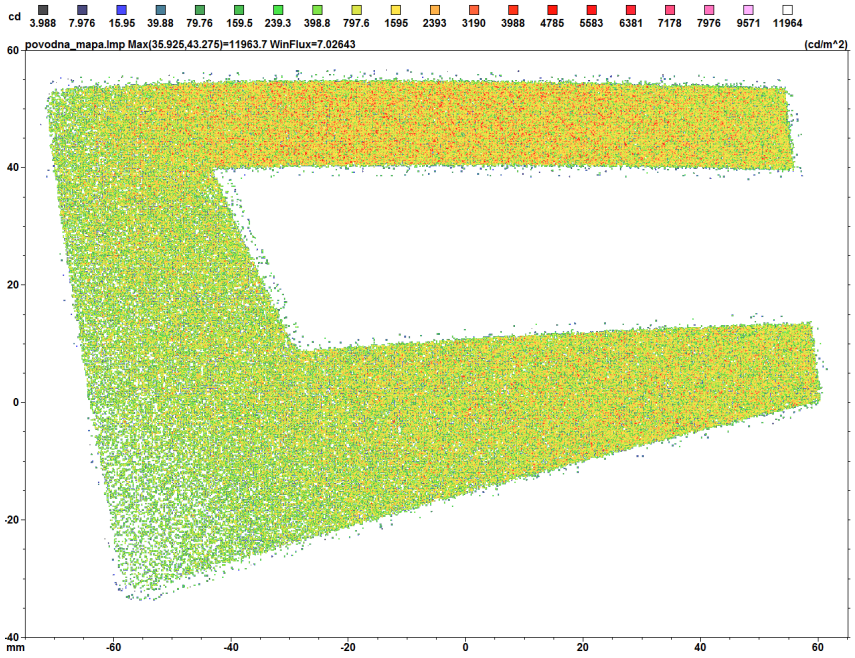

Figure 45: Lit appearance of simulated geometry

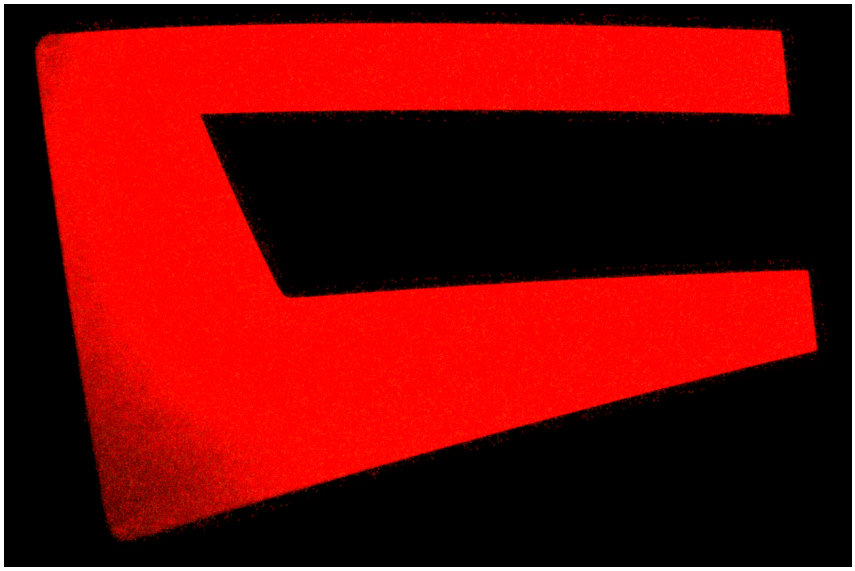

Figure 46: Lit appearance of simulated geometry with Milky filter made in Blender

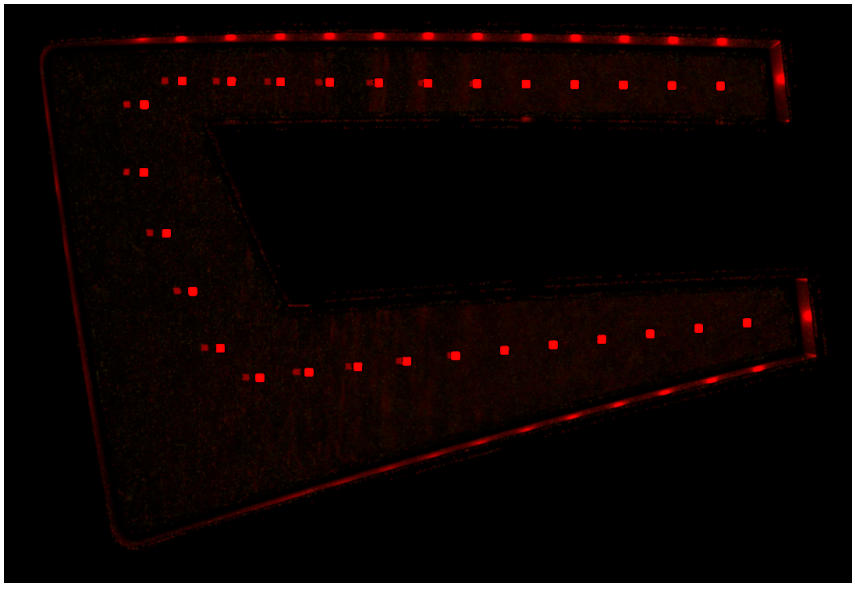

Figure 47: Lit appearance of simulated geometry with transparent filter made in Blender

As it is clear from the figures 46 and 47, Milky filter diffuse emitted light and eliminate hot spots which create LEDs on the transparent filter.

In subsequent part of this chapter will be simulated three different optical elements. After consultations, I decided for the following optical elements: flutes, pillows optics and prism. These optical elements will be placed on surfaces of Milky filter. Detailed descriptions of the individual elements are situated in the following subsections.

7.2 Using flutes on B surface of Milky filter

I have chosen a flutes as the first optical element for the simulations. This optical element is placed on B surface of Milky filter. B surface means the inner side of the filter. Dimensions of this optical element and its position are shown in figure 48. The flutes are optical elements frequently used in automotive lighting for spreading incident light.

Figure 49 shows optical principle of this element. As we can see, spread of light can be controlled by width or radius of the flutes. From this figure is clear that the smaller diameter of flutes cause the higher spread of the light. While placing any optical element on the surface of filter is important to remember, that this optical element shall be visible from the given angle where is needed to make changes of incident light. The figure 50 displays this view (from angle -80 °) on filter with the flutes.

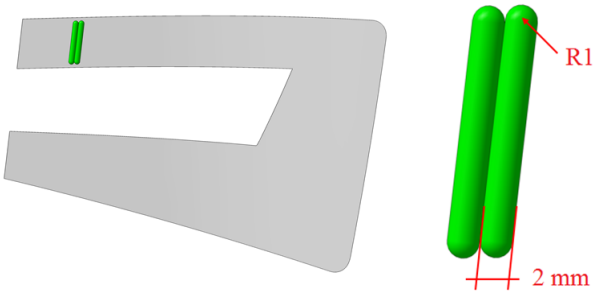

Figure 48: Position and dimensions of flutes placed on B surface of Milky filter

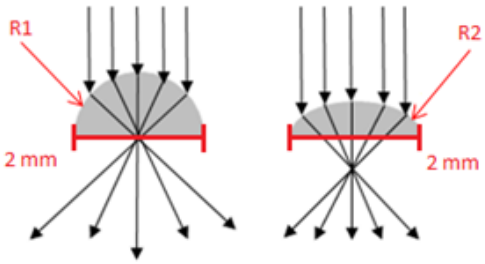

Figure 49: Optical principle of flutes

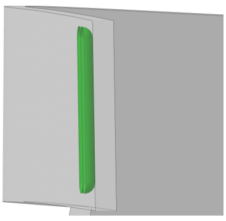

Figure 50: View from -80 °

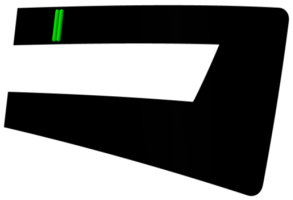

Figure 51: Absorbed layer

The following iso candela maps shows optical principle of flutes. For this simulations was used absorbed layer which transmits only those rays passing through the simulated optical elements (figure 51). The first map in figure 52 shows iso candela map of hole where will be placed optical element. The second picture shows iso candela maps of the flutes with radius R1 and the third picture shows iso candela map of flutes with radius R2. The width of the flutes was 2 mm in both cases. It is clear that the theoretical assumption was confirmed because the flutes with radius R1 spread light much more than the ones with radius R2. Due to higher spread of light of flutes with radius R1, I decided use this shape of flutes for simulations.

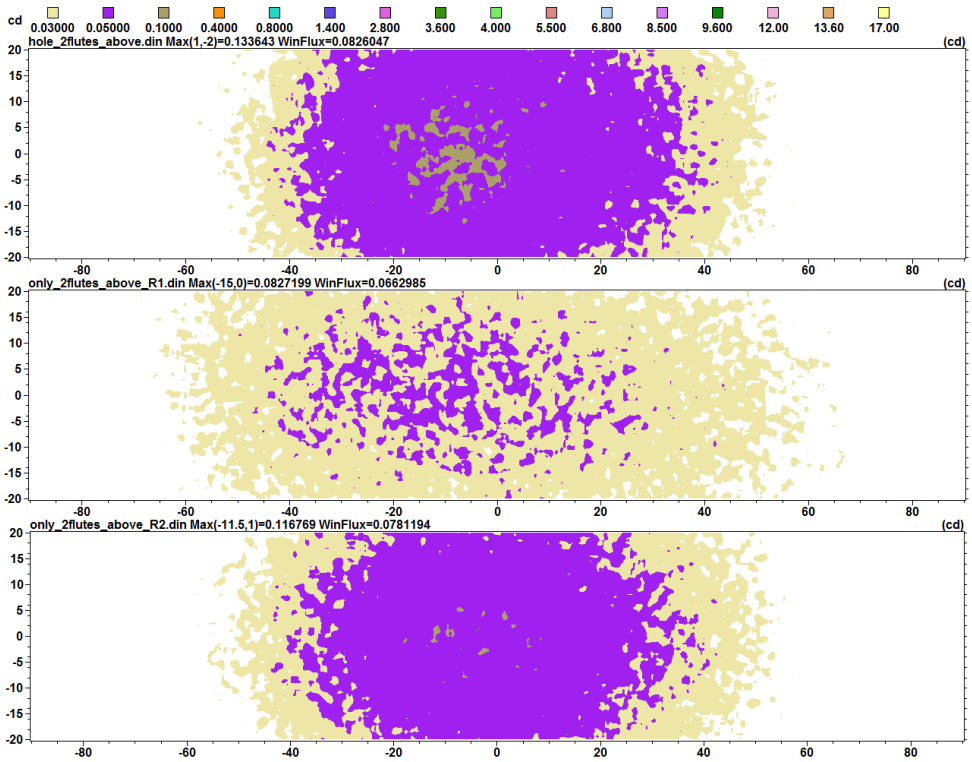

Figure 52: Optical principle of flutes, 1. hole for flutes, 2. Flutes with radius R1 3. Flutes with radius R2

The figure 53 describes differences in optical properties between the flutes made from transparent and Milky material. As we can see from the second iso candela map in figure 53, the light passing through the flutes from Milky material is spread more uniformly than in case with transparent material.

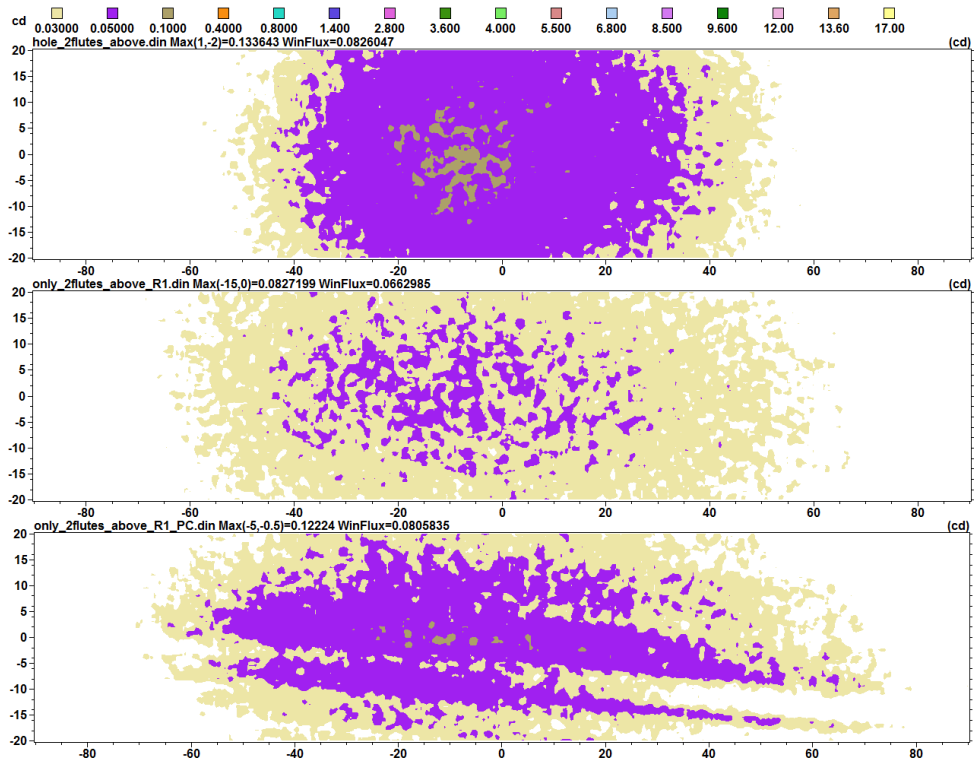

Figure 53: Optical principle of flutes, 1. hole for flutes, 2. Flutes made from Milky material, 3. Flutes made from transparent material

The figure 35 shows iso candela map of origin-simulated geometry (first map) and simulated geometry with using flutes situated on B surface of the filter (second map). From these maps is obvious that the values on the visibility -80 ° have increased about 4% and 5%. However, these values have increased by only a few percent, thus this type of optical element it is not appropriate for solving problem with visibility on -80 °.

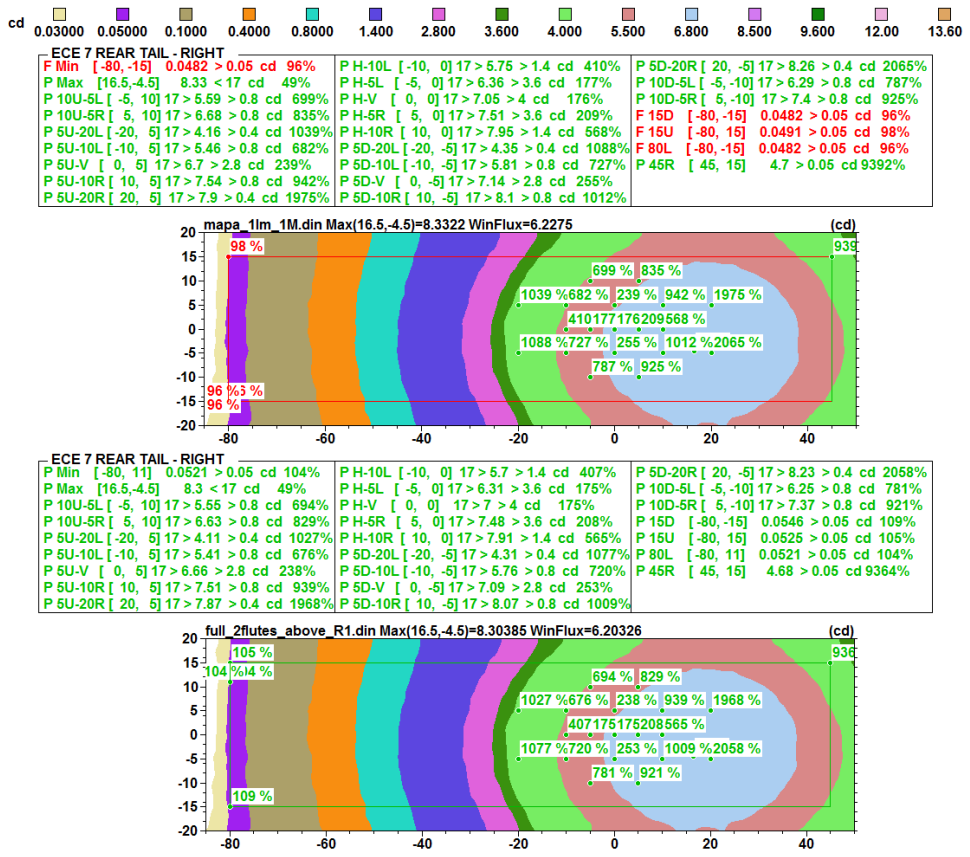

Figure 54: Iso candela map of origin simulated geometry (above) and with using flutes on the Milky filter (bellow)

The figure 55 shows lit appearance of the simulated geometry in false colour. From the picture we can observe an inhomogeneity of lit appearance in position where is placed optical element. At the same time, the figures 56 and 57 show real lit appearance of this geometry created in software LuxRender. The figure 57 shows case with using transparent filter.

In this subsection I simulated optical elements so called flutes which were placed on B surface of Milky filter. As is obvious from the iso candela map (figure 54), this optical element is not appropriate for align the light to the required direction. Due to this reason I decided use for simulations another optical element which will be described in next subsection.

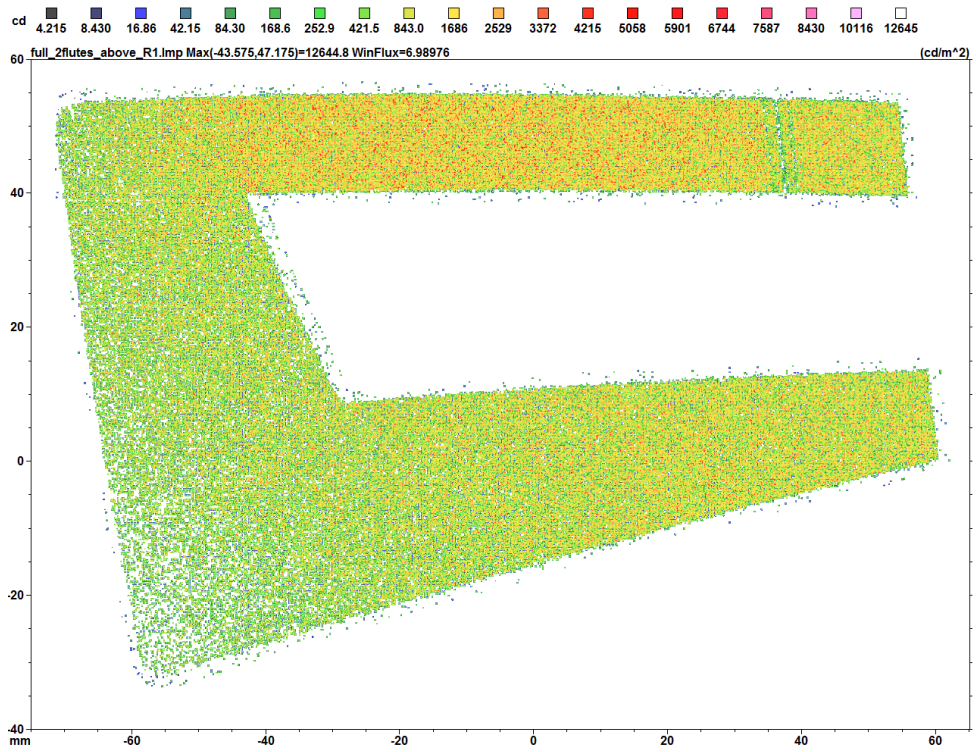

Figure 55: Lit appearance of simulated geometry with using flutes on the Milky filter

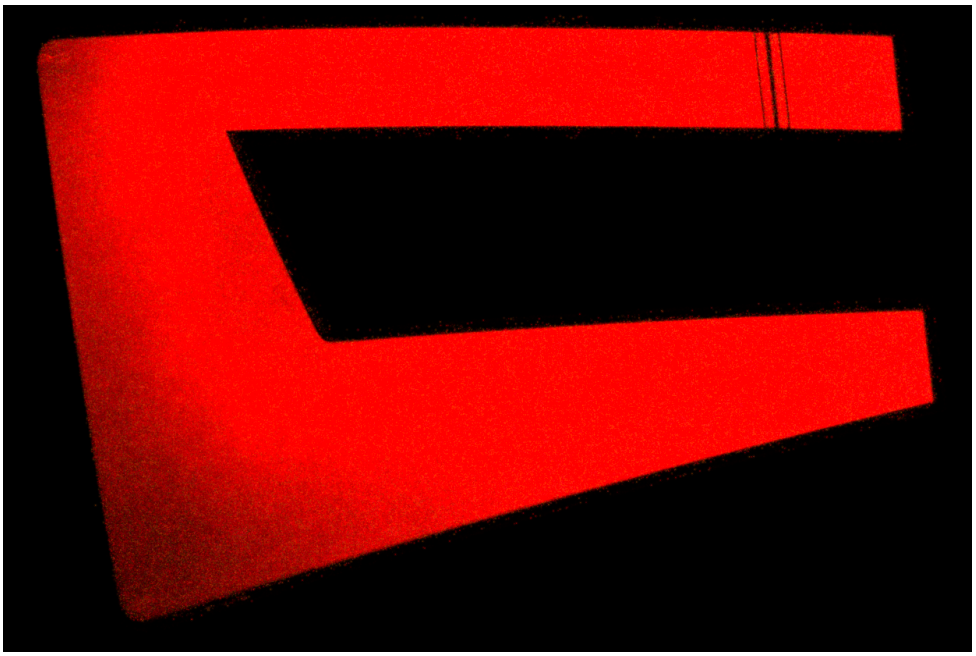

Figure 56: Lit appearance of flutes on Milky filter created in software LuxRender

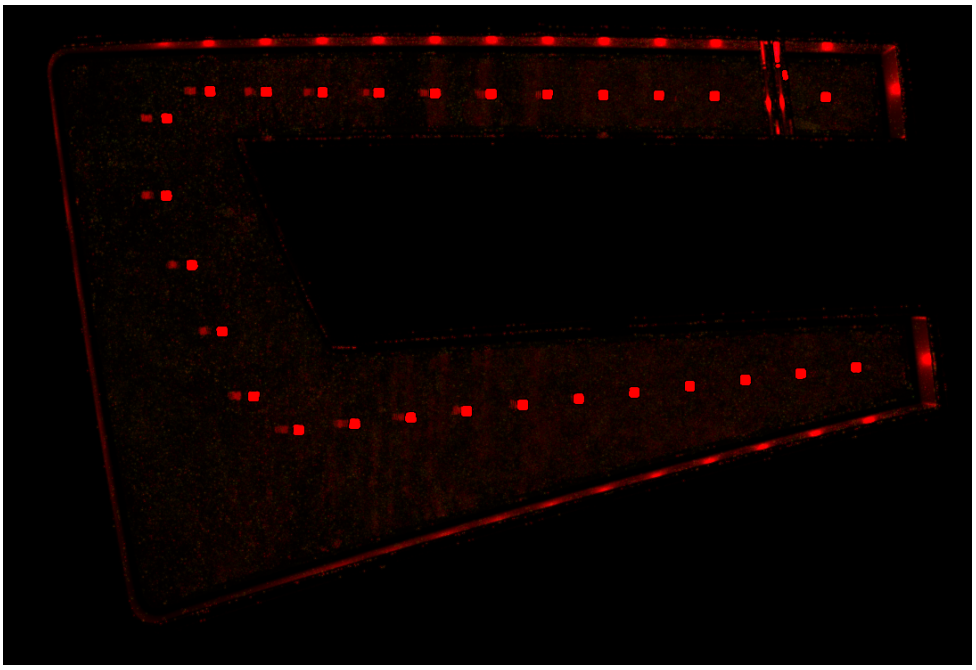

Figure 57: Lit appearance of flutes on transparent filter created in software LuxRender

7.3 Using pillows optics on B surface of Milky filter

This subsection describes simulations of the next optical elements, namely pillow optics, placed on the B surface of Milky filter. The shape and position of this optical element is shown in the figure 58. This optical element is actually composed of several parts (pillows) which can be rotated independently around horizontal and vertical axis. At the same time, it can be set up a parameter so called spread which helps distribute light more to the sides.

Figure 58: Position and shape of optical pillows placed on the B surface of Milky filter

The figure 59 shows iso candela maps of several rotations of pillows. Obviously, the light is the most refracted to the side with using horizontal rotation of pillows -20°. Due to this reason, I decided to use this shape and rotation of pillows for simulations. These iso candela maps was also simulated with using absorb layer like in the previous optical element.

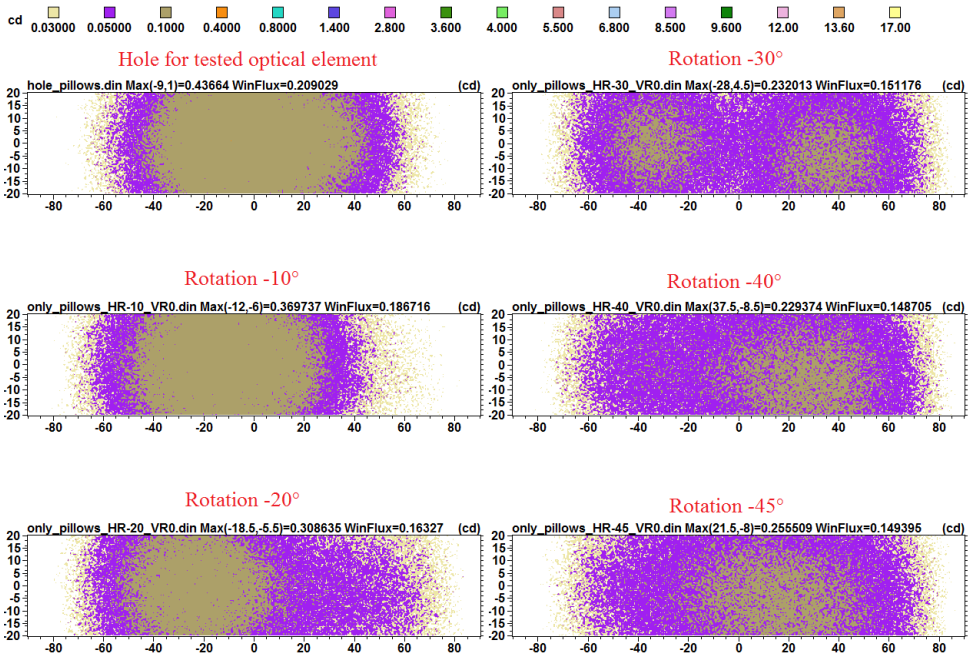

Figure 59: Iso candela maps of several rotation of pillows placed on the Milky filter

The values on the visibility -80 ° have increased by just a few percent as we can see from the iso candela map (figure 60). Apparently, due to the low refraction of light on this shape of pillows optics, it is not appropriate to use this optical element for aligning light to the -80 °. The figures 61,62 show lit appearances of geometry with using pillows optics on B surface of Milky filter. As well as in previous simulated optical elements, we can see inhomogeneity on the position where is placed this element. Lit appearance of this geometry with transparent filter is also shown on the figure 63 for comparison.

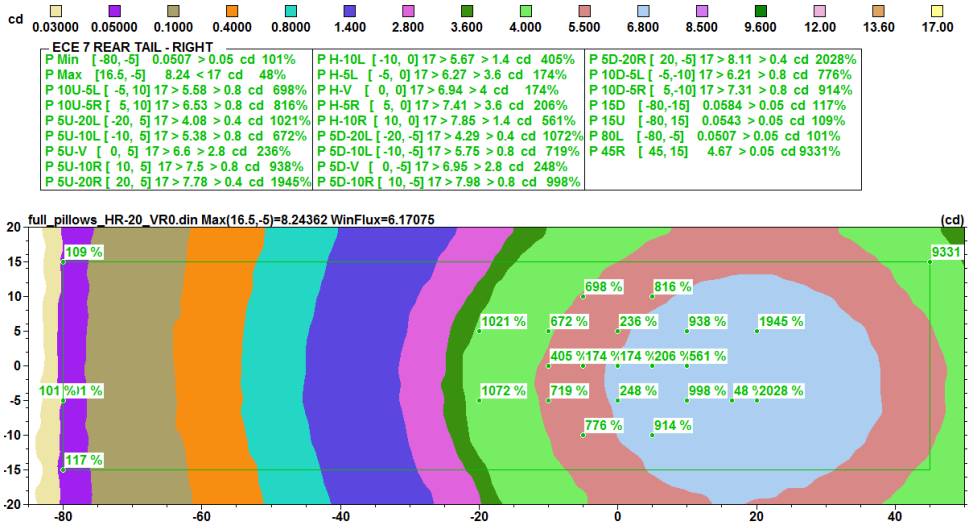

Figure 60: Iso candela map of simulated geometry with using pillows optics on the Milky filter

With regard to the facts mentioned above, I have decided for using next optical element which will be able to align the alight to the required direction. The optical properties of this optical element will be described in next subsection.

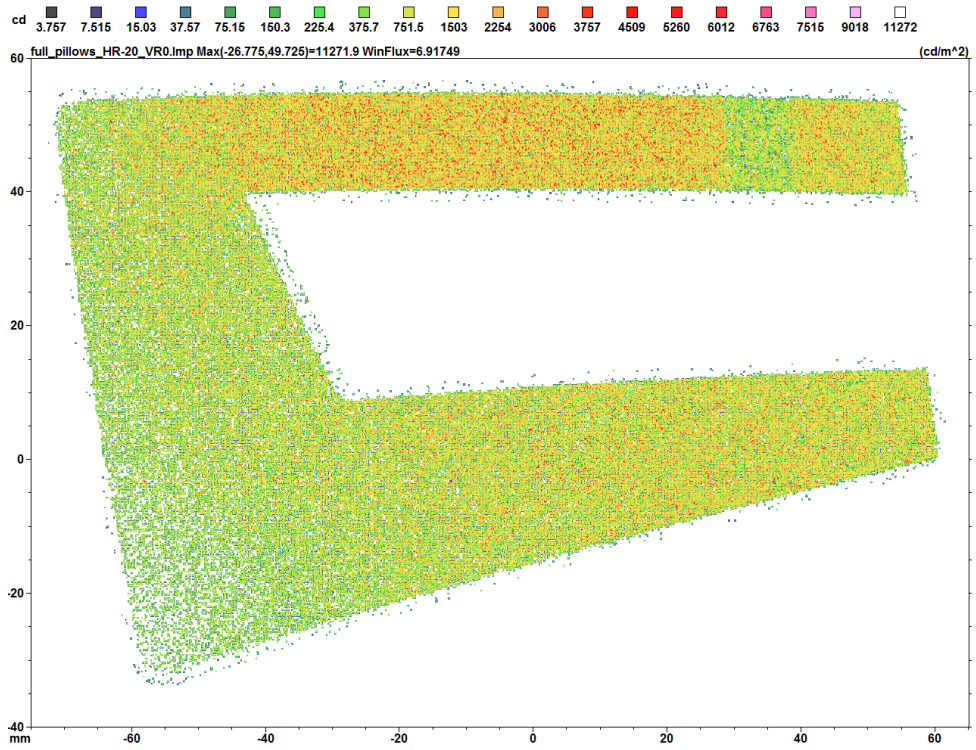

Figure 61: Lit appearance of simulated geometry with using pillows optics on the Milky filter

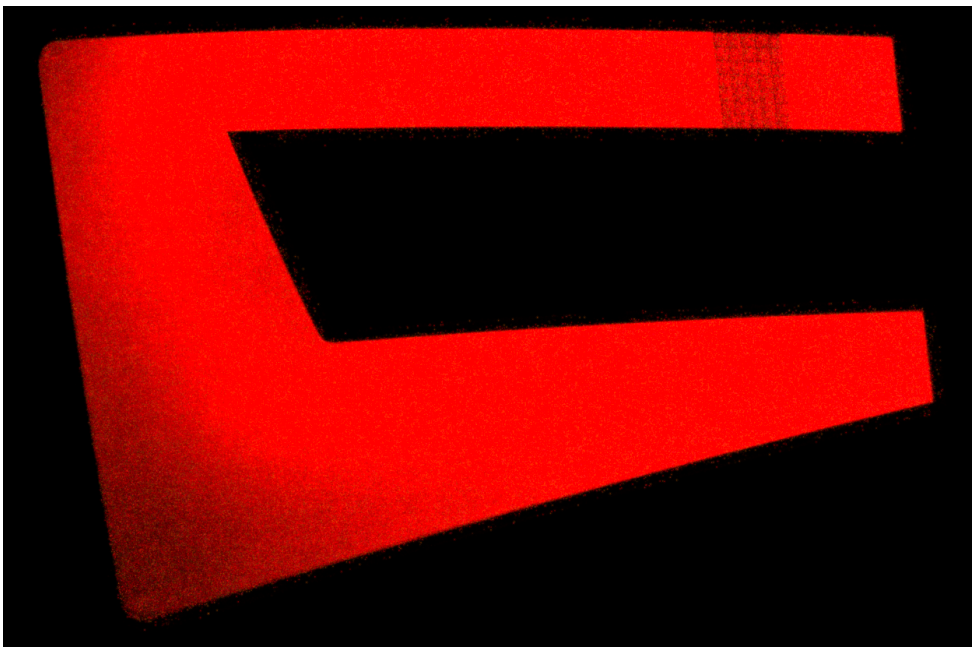

Figure 62: Lit appearance of pillows optics on Milky filter created in software LuxRender

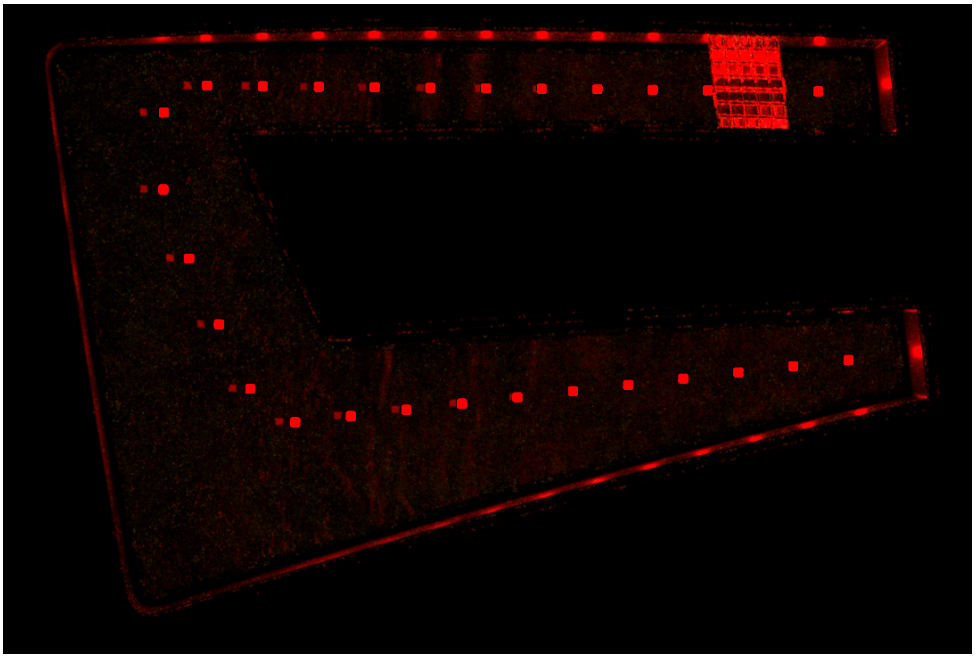

Figure 63: Lit appearance of pillows optics on transparent filter created in software LuxRender

7.4 Using prism on surface of the Milky filter

7.4.1 Prism on B surface of the Milky filter

I have chosen a simple prism as the last optical element for the simulations. This optical element is situated on the B surface of Milky filter as shown in figure 64. B surface means the inner side of the filter. Dimensions of the prism are shown on the right side of the picture.

Figure 64: Dimensions and position of prism, situated on B surface of Milky filter

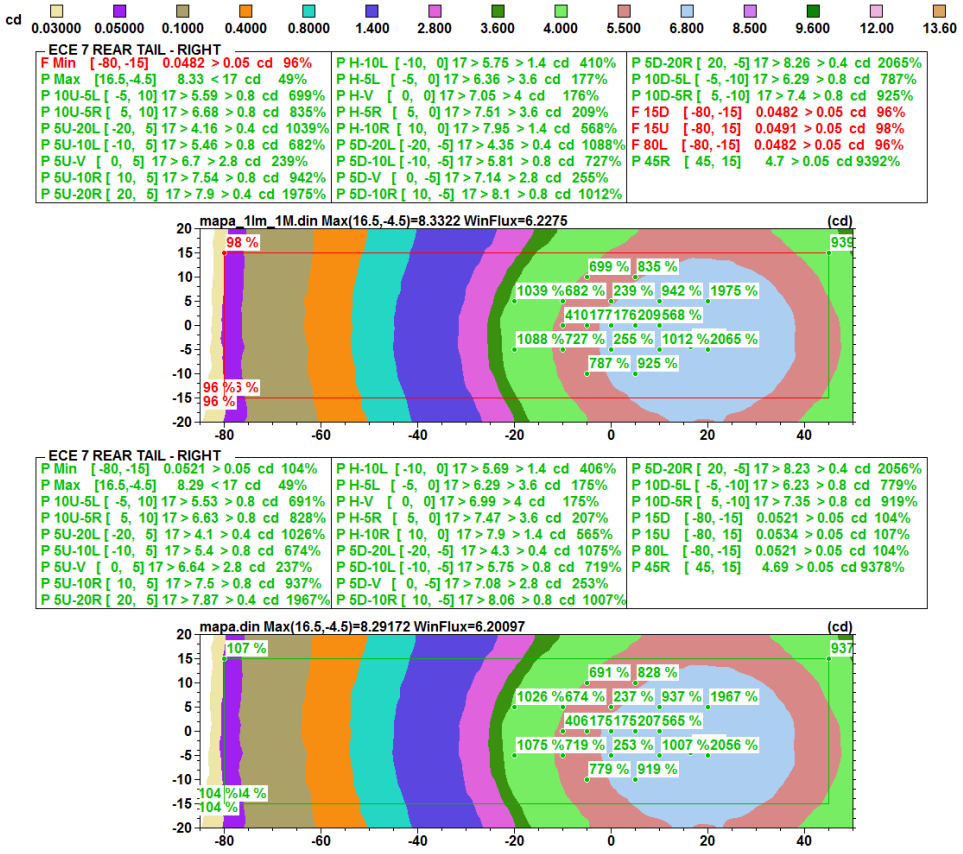

Figure 65: Iso candela map of origin-simulated geomery (above) and geometry with prism situated on B surface of the Milk filter

The figure 65 shows iso candela maps of origin-simulated geometry (above) and simulated geometry with using one prism situated on B surface of filter (bellow). From the picture is obvious that the values on visibility -80 ° have increased after using this optical element. However, these values have increased by only a few percent, thus I decided for using two prisms, which are also situated on B surface of filter.

The figure 66 shows lit appearance of simulated geometry with using one prism on B surface of the filter created in software LightTools. We can see inhomogeneity of lit appearance in position where is placed used optical element at the pictures.

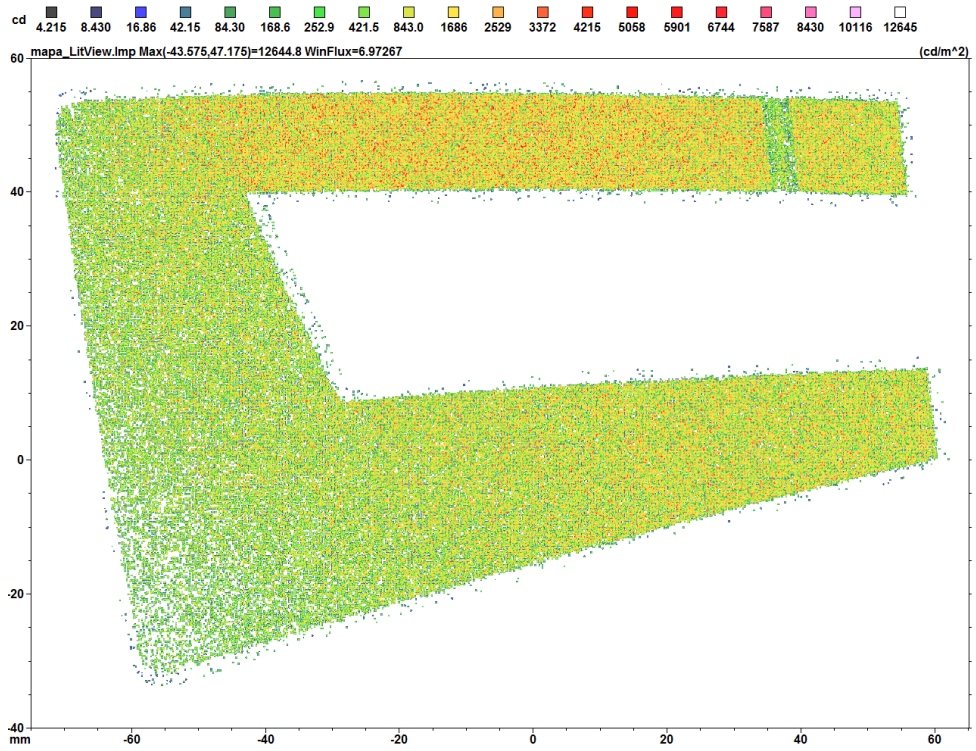

Figure 66: Lit appearance of simulated geometry with one prism on B surface

7.4.2 Two prisms on B surface of the Milky filter

As I have mentioned before, due to low efficiency of using one prism on B surface, I decided for using two prisms also situated on B surface of Milky filter. However, due to the large mass of material, I also changed the dimensions of prism as shows figure 67.

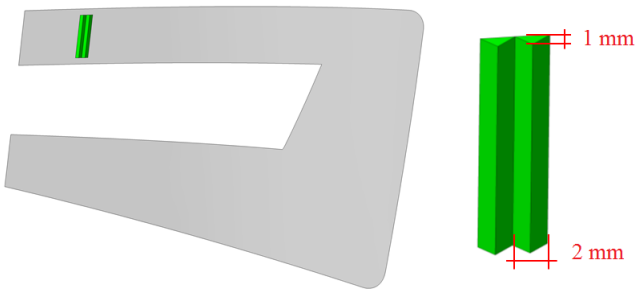

Figure 67: Dimensions and position of two prisms, situated on B surface of Milky filter

Since it is clear from the iso candela maps on the figure 68, the values on visibility -80 ° have not changed, although I used two prisms. This is caused by reducing their size (from 4mm to 2mm). Due to low efficiency of this position of the optical element, I decided for another solution, which describes following subsection.

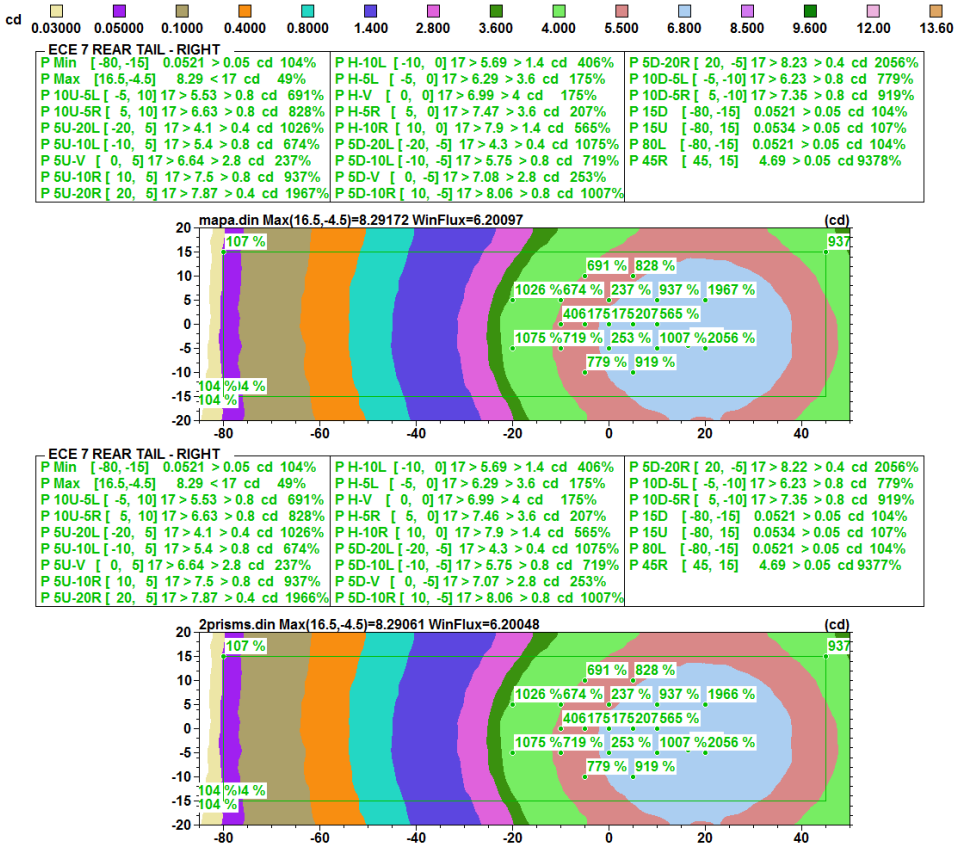

Figure 68: Iso candela maps of geometry with using one prism (above) and using two prisms (bellow) on B surface of Milky filter

In the figures 69, 70 are shown lit appearances of this geometry. Apparently there is an inhomogeneity on the position where is placed optical element. For comparison, lit appearance of transparent material among different materials is also demonstrated (figure 71).

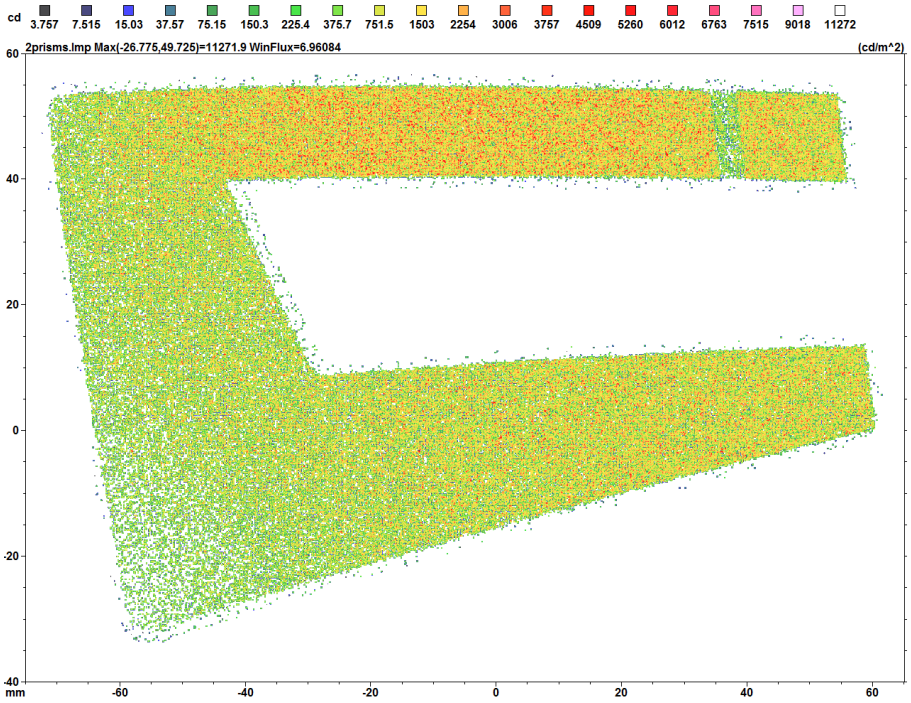

Figure 69: Lit appearance of geometry with two prisms on B surface of Milky filter

Figure 70: Lit appearance of geometry with using one prism on B surface of Milky filter

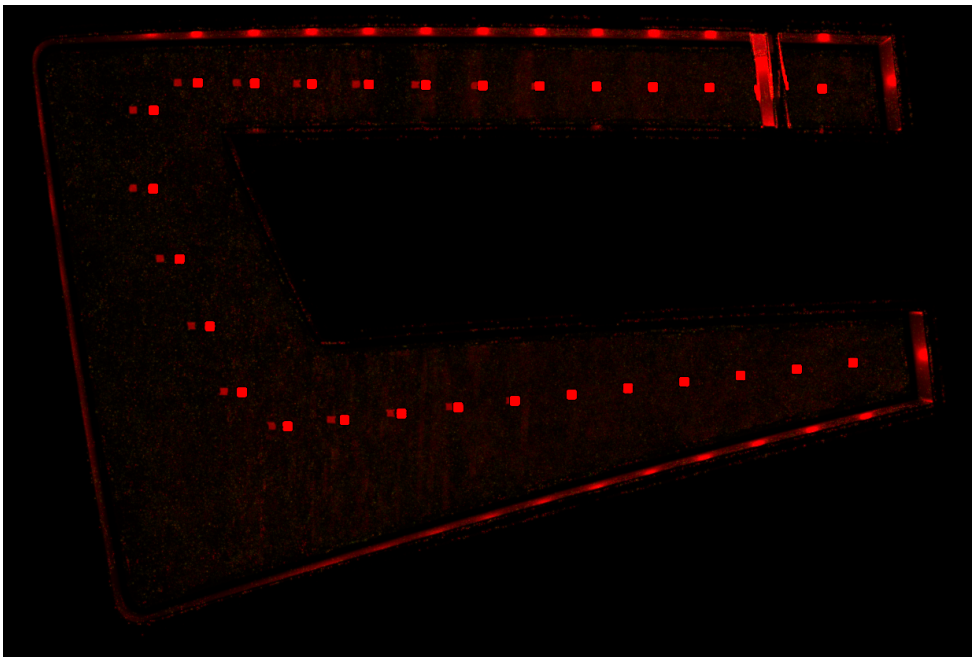

Figure 71: Lit appearance of geomery with using one prism on B surface of transparent filter

7.4.3 One prism on A surface of the Milky filter

Due to low efficiency of prism placed on B surface of Milky filter, I decided for placing this shape of optical element on A surface. A surface means the outer side of the filter. The figure 72 shows principle of this optical element and effect of orientation and position on its optical properties. The first picture shows principle of prism placed on B surface of filter. As we can see, according to Snell's law, ray of light which impacts on the first interface is refracted towards normal and after impacts on the second interface is refracted away from the normal. Otherwise, in the second case where prism is oriented on the A surface of filter, situation is completely different. As we can see, the ray of light is reflected on the first interface according to total internal reflection and subsequently is refracted away from the normal. As seen from the pictures, the placing prism on A surface is much efficient because the light in the second case is more refracted to the side. This theoretical assumption neglects ideal case where is the incident ray reflected back (principle of reflex reflector). The picture 73 shows position and dimensions of this prism placed on the A surface of the Milky filter.

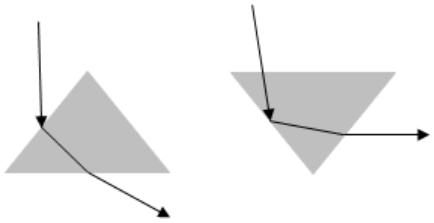

Figure 72: Optical principle of prism on B surface (left) and on the A surface (right)

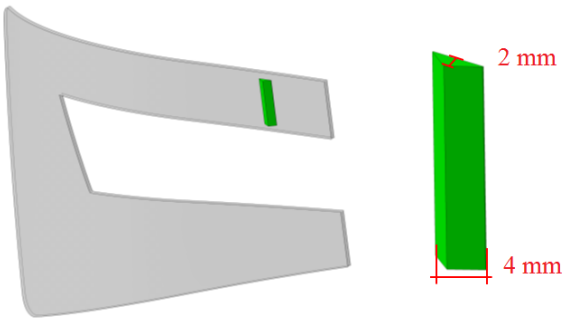

Figure 73: Dimensions and position of prism, situated on A surface of Milky filter

As is obvious from the iso candela maps (figure 74), prism situated on the A surface is more efficiency as prism situated on the B surface. As we can see, the values on visibility -80 ° have increased about 23% and 31%. Figures 75 and 76 show lit appearances of geometry with this optical element and it is clear that homogeneity in case of prism situated on A surface is much better than in case of prism placed on B surface (figure 69). Lit appearance of geometry with transparent filter is also shown on the figure 77 for comparison.

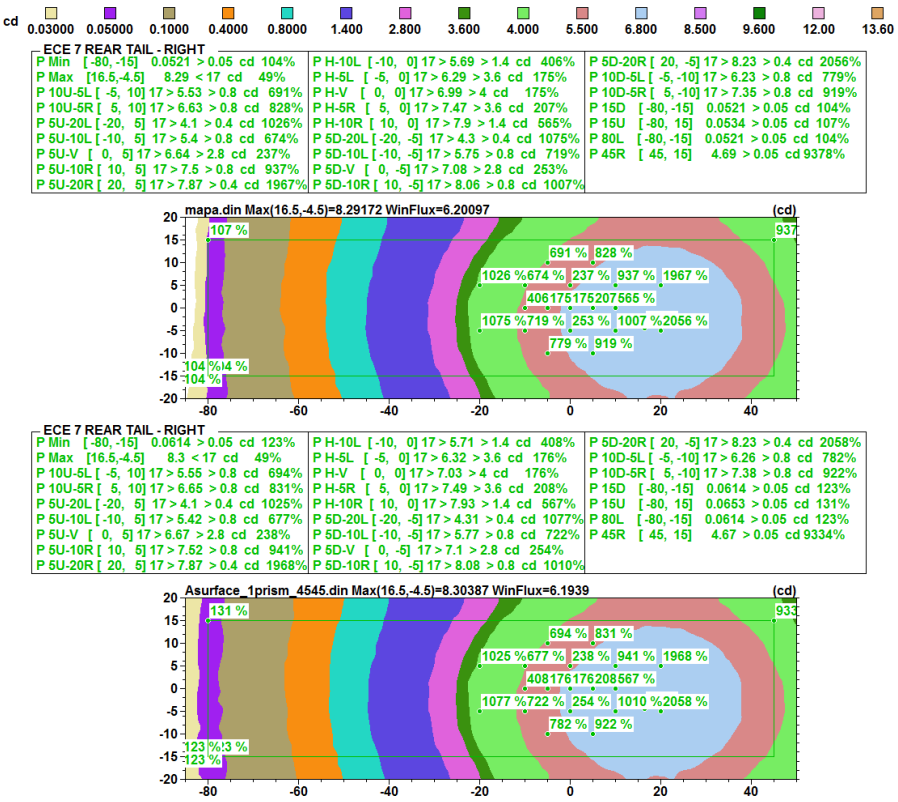

Figure 74: Iso candela map of simulated geometry with prism situated on B surface (above) and on A surface (bellow) of Milky filter

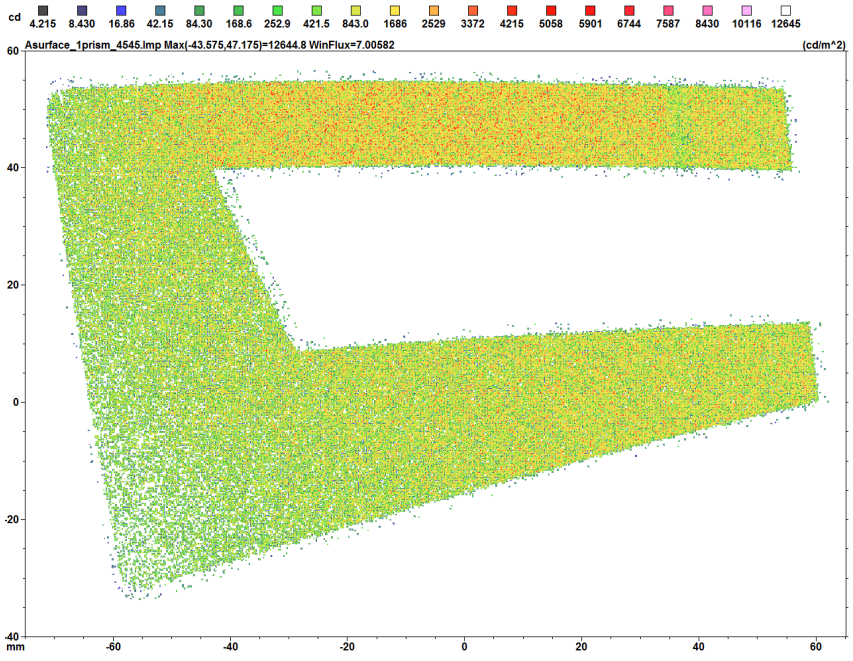

Figure 75: Lit appearance of simulated geometry with prism situated on A surface of Milky filter

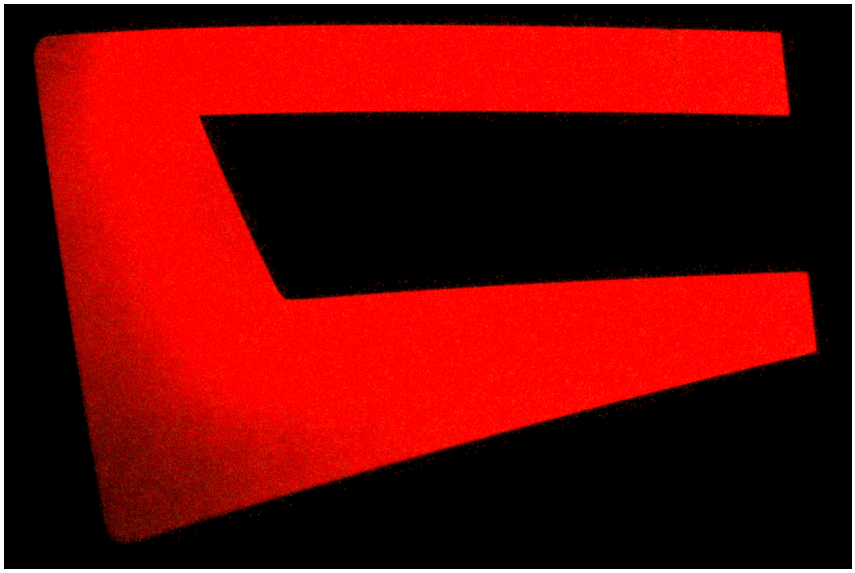

Figure 76: Lit appearance of prism situated on A surface of Milky filter created in software LuxRender

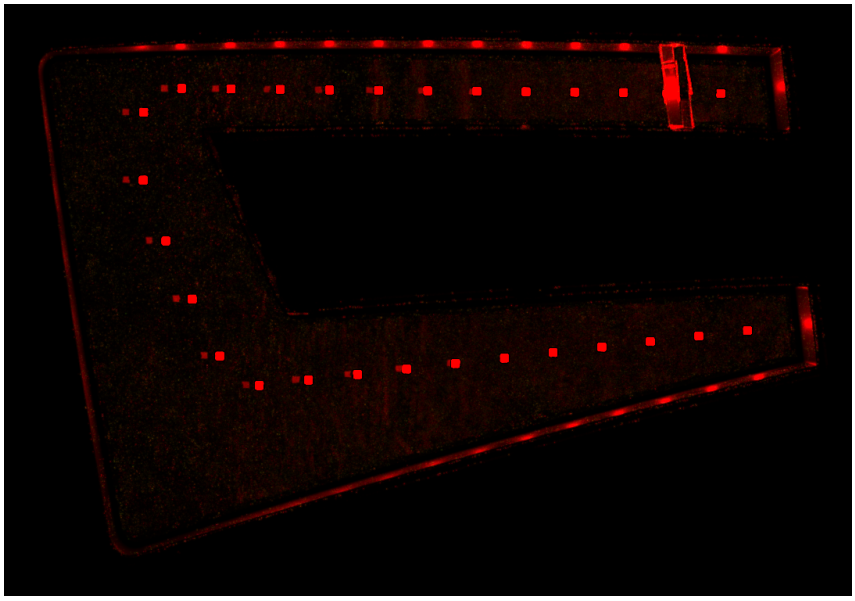

Figure 77: Lit appearance of prism situated on A surface of transparent filter created in software LuxRender

7.4.4 Comparison of type of materials

This subsection describes differences between optical properties of Milky and transparent materials. Figure 80 indicates iso candela maps for situation without any optical element (first map), situation with using Milky material (second map) and situation with using transparent material. With regard the figure 79 is clear that for the simulation of optical properties is used absorb layer, which is offseted from the filter about 0.1 mm. This layer transmits only those rays that pass through the simulated optical elements.

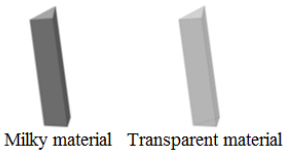

Figure 78: Types of material

Figure 79: Absorbed layer

The first case in the figure 80 shows iso candela map just for hole, where will be situated optical elements. The second case shows iso candela map for rays which are passed through Milky prism. We can see that part of rays are refracted to the sides and a lot of rays passes directly through to prism. From the figure is also evident that rays passes through Milky filter are diffused. Otherwise, rays which passes through transparent prism are just reflacted to the sides, however without any diffuse effect. This experiment confirms theoretical assumption.

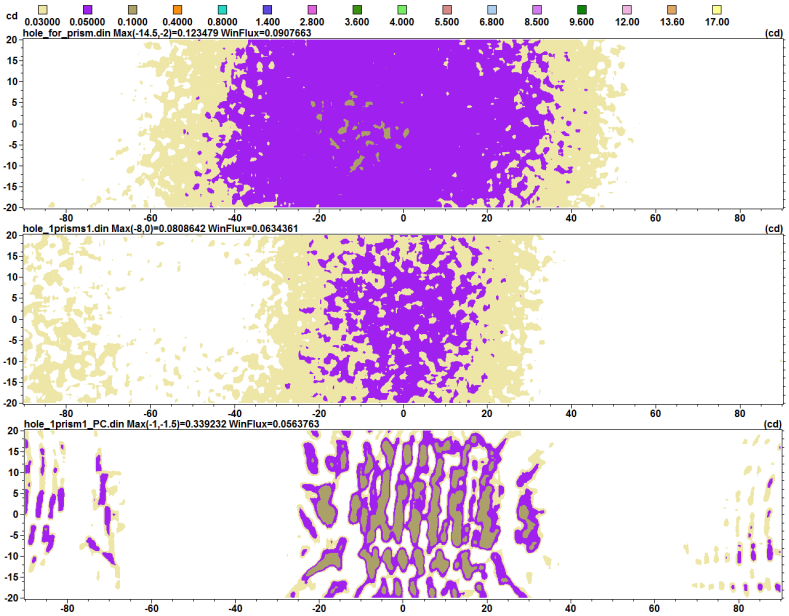

Figure 80: Iso candela maps for different types of material: 1-hole for element, 2-prism from Milky material, 3-prism from transparent material

7.4.5 Comparison of shape of prism

In the previous subsection were explained differences between optical properties of Milky and transparent materials whereas this subsection describes optical properties of the different shapes of prism. As it is obvious from the figure 81, the rays passing through the second type of prism are refracted much more as in the first case. On the grounds of this reason is this shape of optical element used for next simulations.

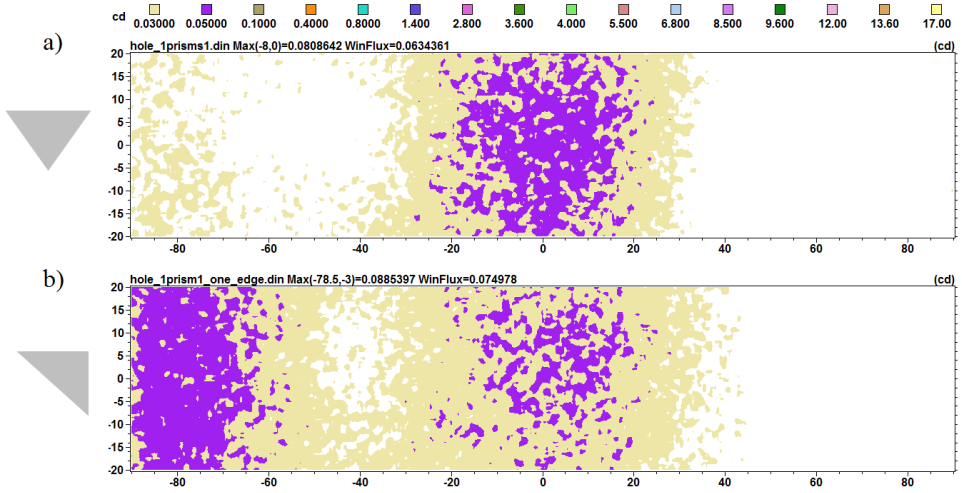

Figure 81: Comparison of different shape of prism situated on A surface of filter

7.4.6 Using special shape of prism on A surface of the Milky filter

On the basis of what have been already explained in the previous subsection, due to high efficiency of the shape of prism showed on the figure 81 b, this element is used for next simulations. Figure 82 shows position and dimensions of this optical element. With regard the iso candela map shown in figure 82, the values on the visibility -80 ° have increased from previous shape of prism. Figure 83 shows lit appearance of using this optical element on A surface of Milky filter. As in previous simulations, we can see inhomogeneity on place where is situated optical element.

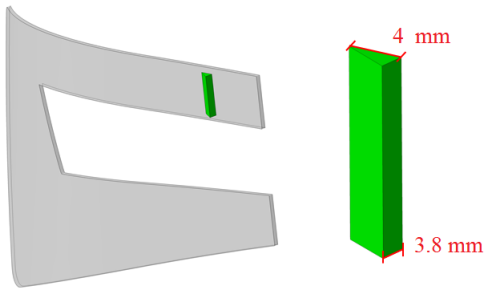

Figure 82: Dimensions and position of special shafe of prism, situated on A surface of Milky filter

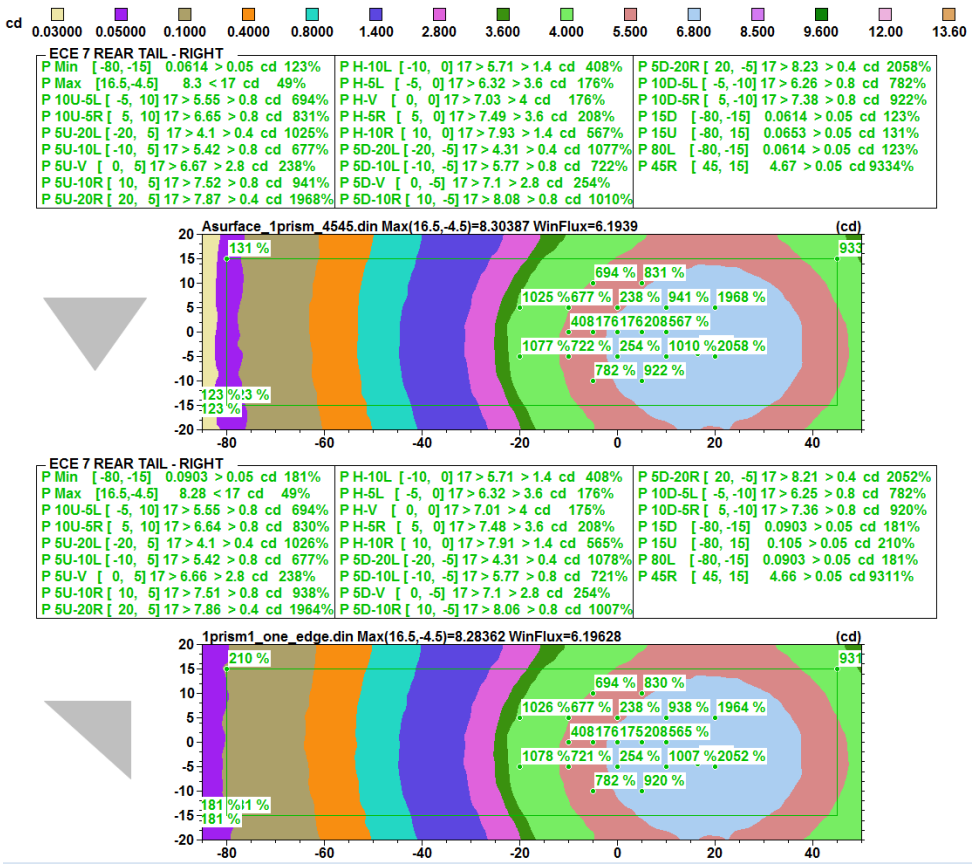

Figure 83: Iso candela map of simulated geometry with improved prism situated on A surface

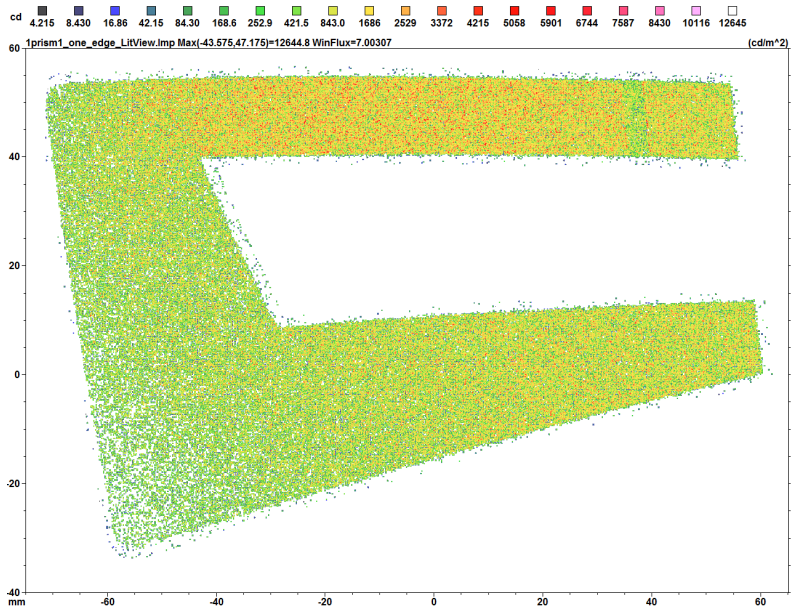

Figure 84: Lit appearance of simulated geometry with improved prism situated on A surface

For better evaluation of homogeneity is also shown lit appearance created in LuxRender (figure 85). Figure 86 indicates lit appearance with using transparent filter.

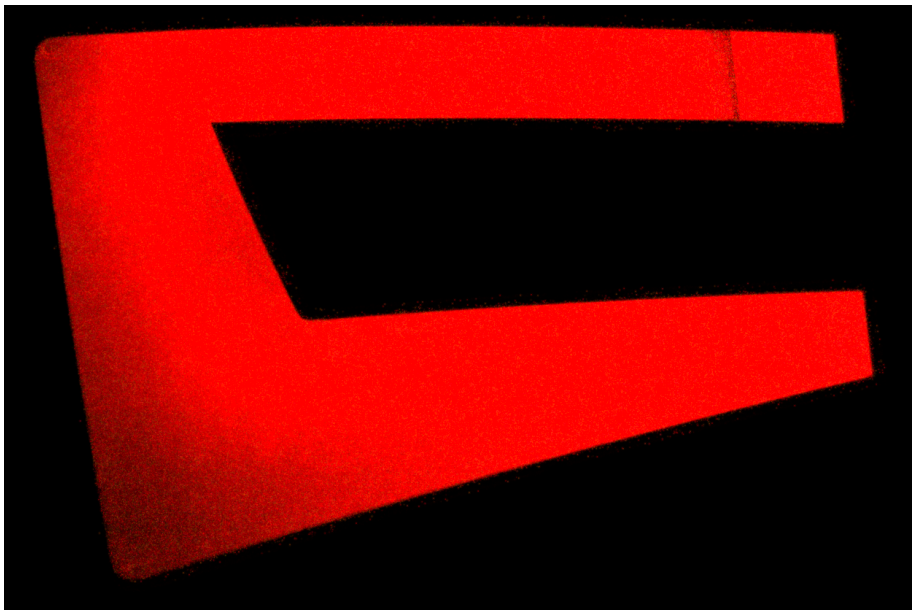

Figure 85: Lit appearance of the second type of prism situated on A surface of Milky filter created in software LuxRender

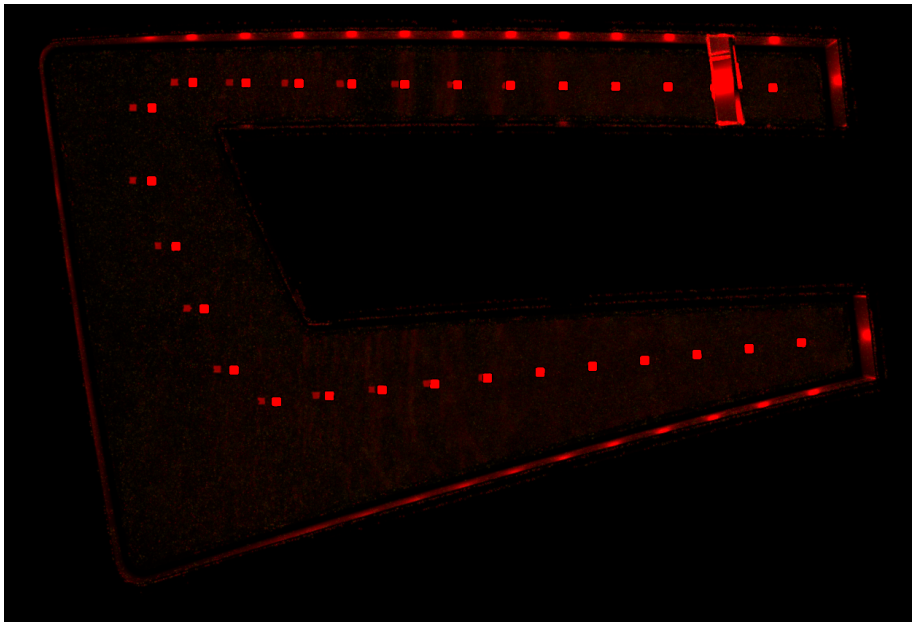

Figure 86: Lit appearance of the second type of prism situated on A surface of transparent filter created in software LuxRender

7.4.7 Upgrading prism on A surface - 4 mm spacing, near the edge

Although the shape of prism described in the previous subsection has big efficiency, due to aesthetic function of whole lamp I decided to place this optical element on the right side of the Milky filter as shows figure 87. The dimensions of this optical element remain the same as in the previous example.

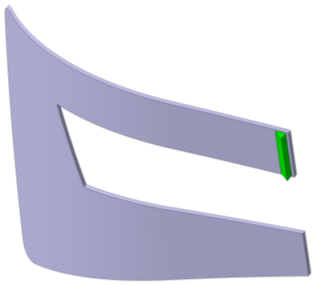

Figure 87: Position of prism situated near edge of A surface of Milky filter

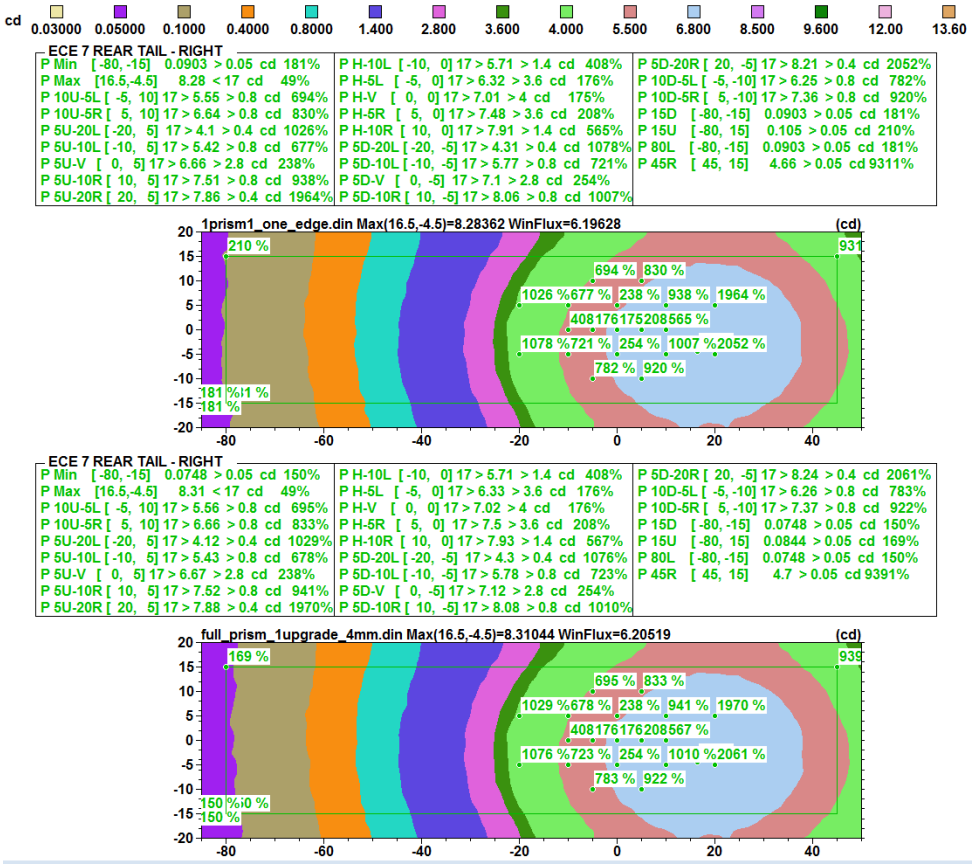

Figure 88: Iso candela maps of simulated geometry with improved prism with origin position (above) and situated on the edge of A surface (below) of Milky filter

As we can see from the iso candela map (figure 88), the values on the visibility -80 ° have decreased by changing of prism position, however values still meet the standard. As we can see from the figure 87, the dimension of prism is large, thus filter cannot be made by molding process. Due to this reason, I decided to reduce dimensions of this optical element in the subsection.

The figure 89 shows lit appearance of this prism position. From this lit appearance is obvious that is much better to place optical element near edge of the filter for the aesthetic function.

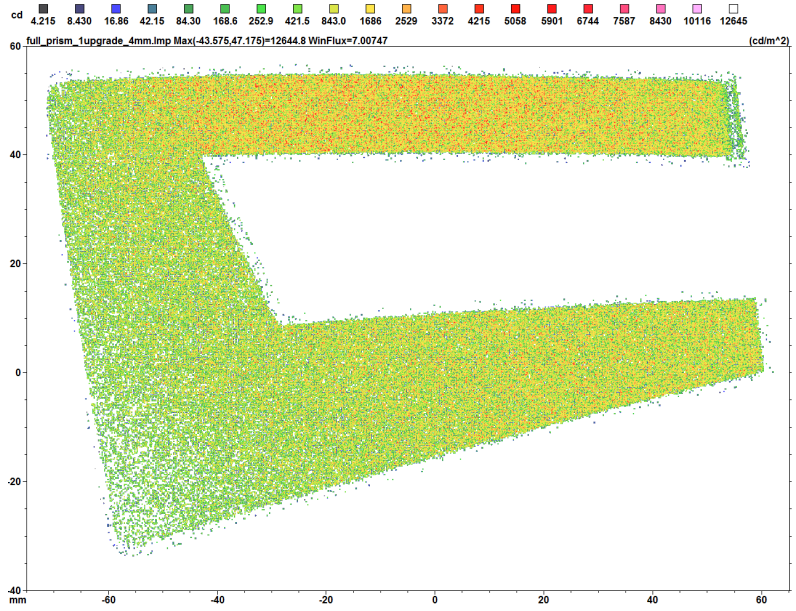

Figure 89: Lit appearance of simulated geometry with improved prism situated on the edge of A surface of Milky filter

7.4.8 Upgrading prism on A surface - 2 mm spacing, near the edge

As I have mentioned in the previous subsection, due to large mass of material, I decided to reduce dimensions of simulated optical element. These dimensions are shown in the right side of the figure 90.

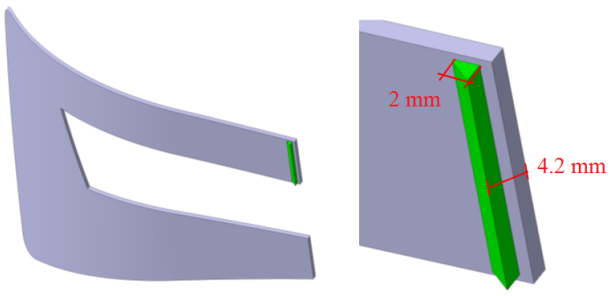

Figure 90: Dimensions and position of prism, situated on the edge of A surface of Milky filter

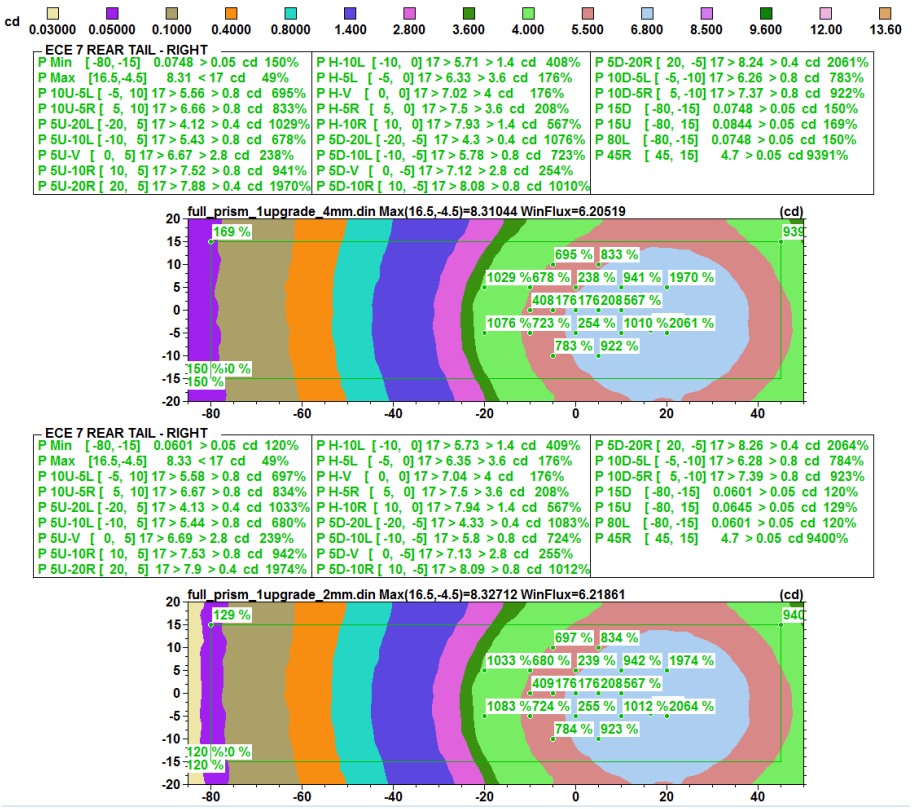

Figure 91: Iso candela map of simulated geometry before reducing dimensions (above) and after reducing dimension (bellow) of prism situated on the edge of A surface of Milky filter

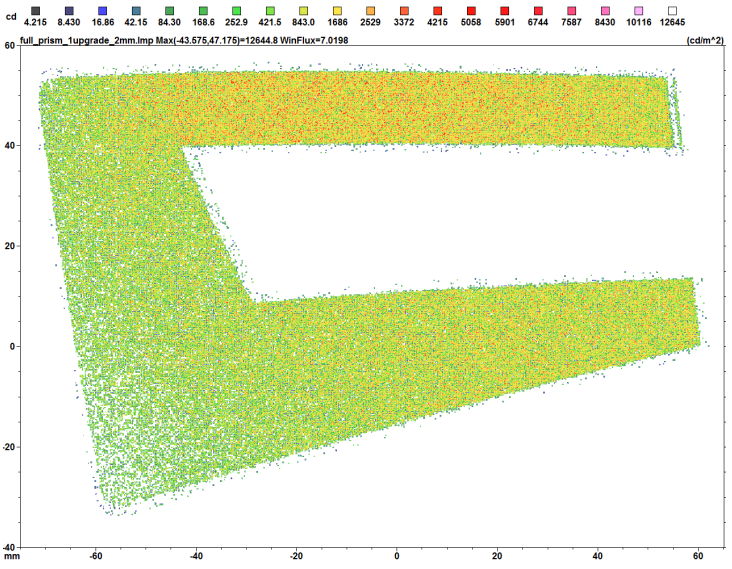

Figure 92: Lit appearance of simulated geometry with reducing dimension of prism situated on the edge of A surface of Milky filter

The figures 92, 93 and 94 show lit appearances of the final position and dimensions of prism. From these lit appearances is clear that for aesthetic function of lamp is much better smaller dimensions and placing of optical element near the edge of the filter.

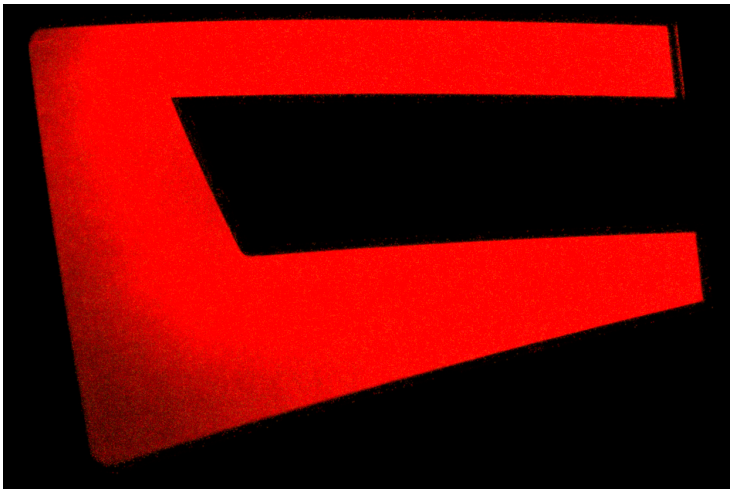

Figure 93: Lit appearance of the improved prism situated on the edge of A surface of Milky filter created in software LuxRender

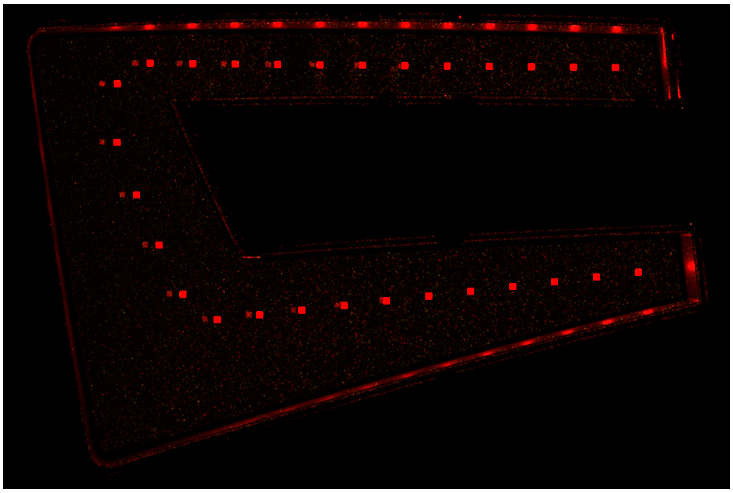

Figure 94: Lit appearance of the improved prism situated on the edge of A surface of transparent filter created in software LuxRender

In these subsections, I simulated optical properties of prism with different dimensions, situated on the several positions of Milky filter. I started with placing this optical element on the B surface of the filter. However, due to low efficiency of prism situated on this surface of filter, I decided to place prism on outer side of the filter (A surface). As is clear from the iso candela maps (figure 65), this position of optical element has much more efficiency. However, due to aesthetic function and production technology I had to change a position of this optical element and reduce its dimensions as well. The final version of this optical element placed on the Milky filter is described in the subsection 7.4.8. However, the thickness of the final filter with optical element is still 4.2 mm, what is on the border of manufacturability. At the same time homogeneity of lit appearance is not good after using optical element on A or B surface of the filter, thus it does not meet the aesthetic function of rear lamp. The results from these subsections suggest that with using prism on the surface of Milky filter it is possible to align a light to the required directions. However, positioning of the optical element on the surface of Milky filter significantly impairs homogeneity of the emitted light, thus it is not possible meet the aesthetic and stylistic function of the lamp.

8 Simulation of proposed optical system from Milky material

In the previous chapter, I have described process of simulation of optical properties for different optical element. This chapter is dedicated to the simulations where I tried to move the maximum intensity to the H-V point in iso candela map. I decided used the same pillows optics like in the subsection 7.3, but I created this optics on entire B surface of Milky filter for meet this purpose. It is obvious from the figure 95 that the pillows optics is placed on entire surface except the edges where is located tube of mirror.

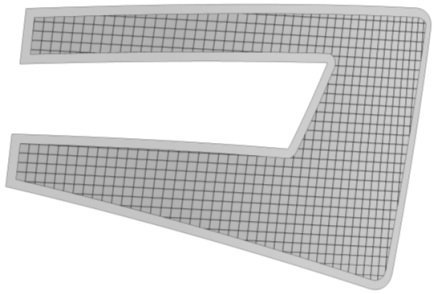

Figure 95: Pillows optics on entire B surface of the filter

The figure 96 shows iso candela map of pillows optics placed on B surface of Milky filter without any rotation of the elements. As we can see from this iso candela map, the maximum intensity in this geometry is located in point [17, -4.5], thus I had to refract the emitted light more to the left and up. With regard this fact I have rotated pillows about 20 ° to the left in the first step of my simulation.

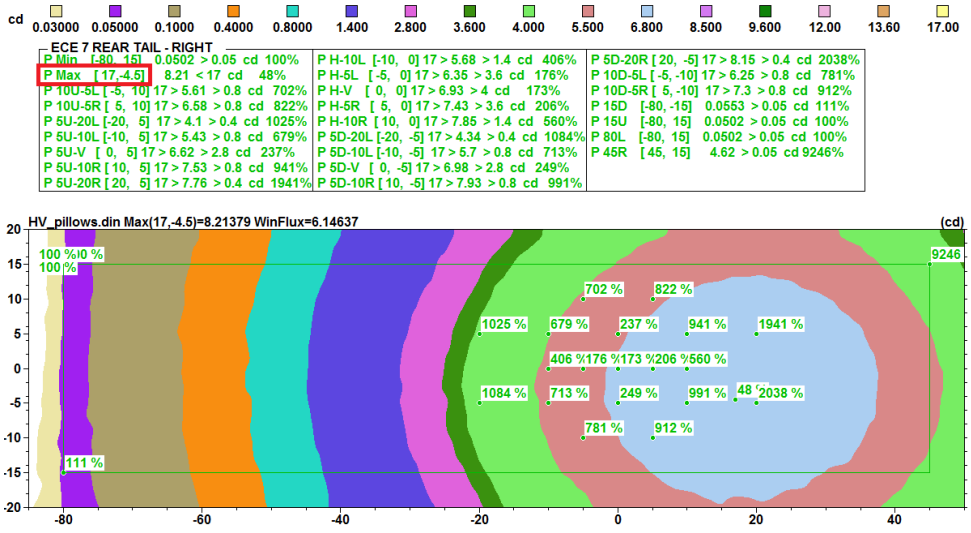

Figure 96: Iso candela map of simulated geometry with pillows optic on entire B surface of Milky filter without any rotations

According to the following iso candela map (figure 97), the point with maximum of intensity after this modification has been moved to the point [2.5,-2.5]. Subsequently, I have rotated pillows optics about 5 ° up. The iso candela map with the point of maximal intensity after this rotation is shown in the figure 98. As is clear from this iso candela map, the maximum of intensity is after that much closer to H-V point [-0.5, 2.5].

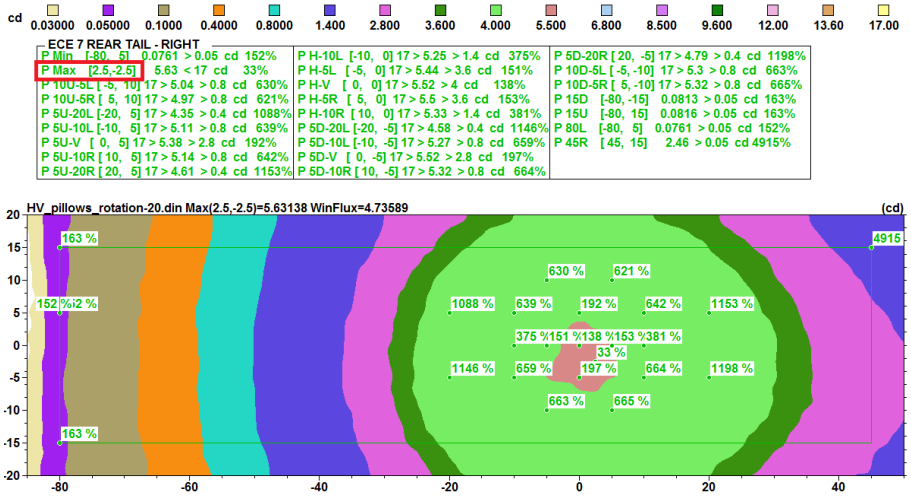

Figure 97: Iso candela map of pillows optics with rotation of pillows about -20 ° horizontally.

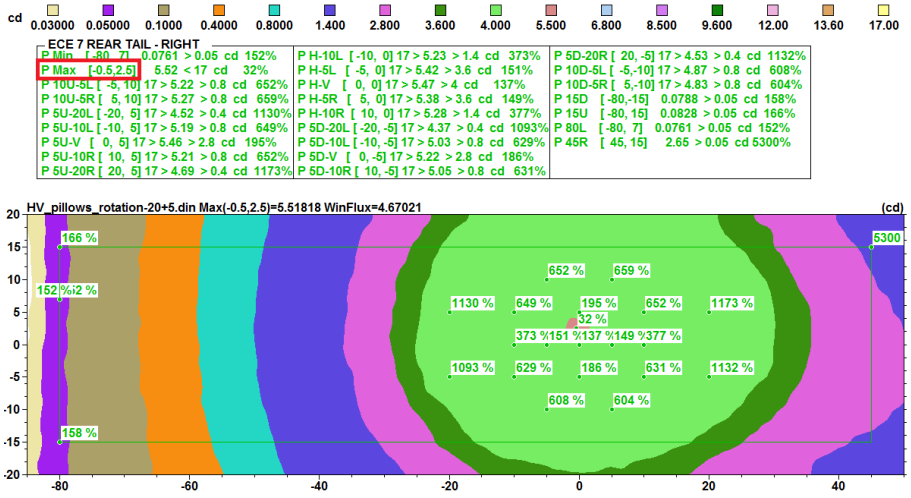

Figure 98: Iso candela map of pillows optics on with rotation of pillows about -20 ° horizontally and +5 ° vertically

As a next step of the simulation, I have not moved with individual pillows, however I have shifted entire surface of pillows optics to the forward direction about 0.1 mm. As it is obvious from the iso candela map (figure 99), the maximum of intensity after this step has moved again much more to the H-V point [0, 1.5]. Given that the maximum of intensity is almost in H-V point, it was the last step in the simulations.

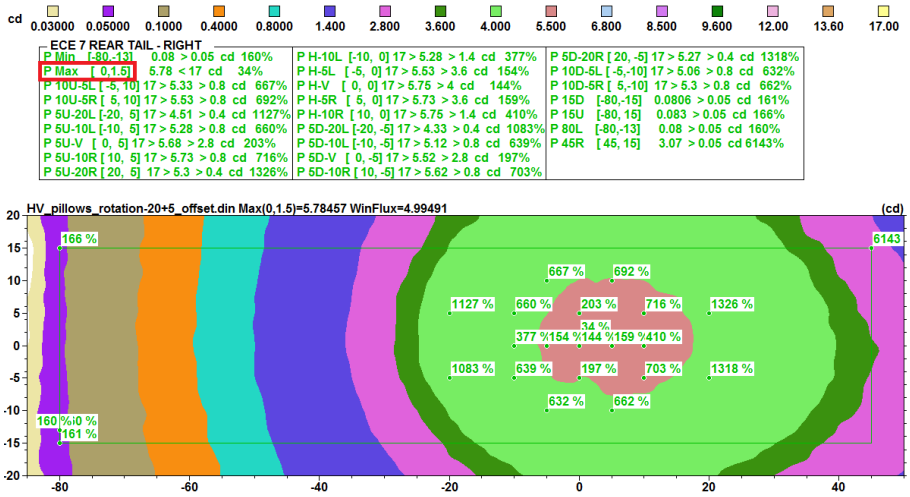

Figure 99: Iso candela map of pillows optics on Milky filter with rotation of pillows about -20 ° horizontally and +5 ° vertically and with offset 0.1 mm forward

The picture 100 demonstrates the fact that each part of pillows optics can be rotated separately. In this case, pillows in red rectangle are rotated -20 ° horizontally and -5 ° vertically, pillows in yellow rectangle are rotated just -20 ° horizontally, and pillows in black rectangle are rotated -20 ° horizontally and +5 ° vertically. Iso candela map from this simulation is shown in figure 101.

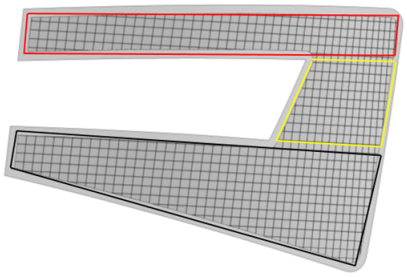

Figure 100: Demonstration of rotation of pillows

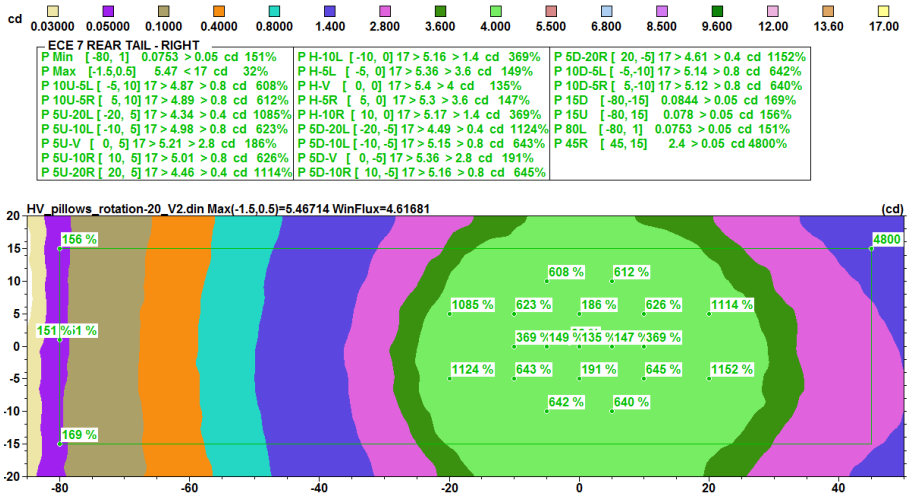

Figure 101: Iso candela map of demonstration of rotation of pillows

In the following pictures we can see lit appearances of simulated geometry with pillows optics without any rotation of pillows (figure 102) and with rotation of pillows -20 ° horizontally a +5 ° vertically (figure 103). We can observe differences in homogeneity among them. While homogeneity of pillows optics without rotation stayed almost the same like in origin geometry, homogeneity of rotated optics has change to worse. We can see inhomogeneities created by the individual pillows.

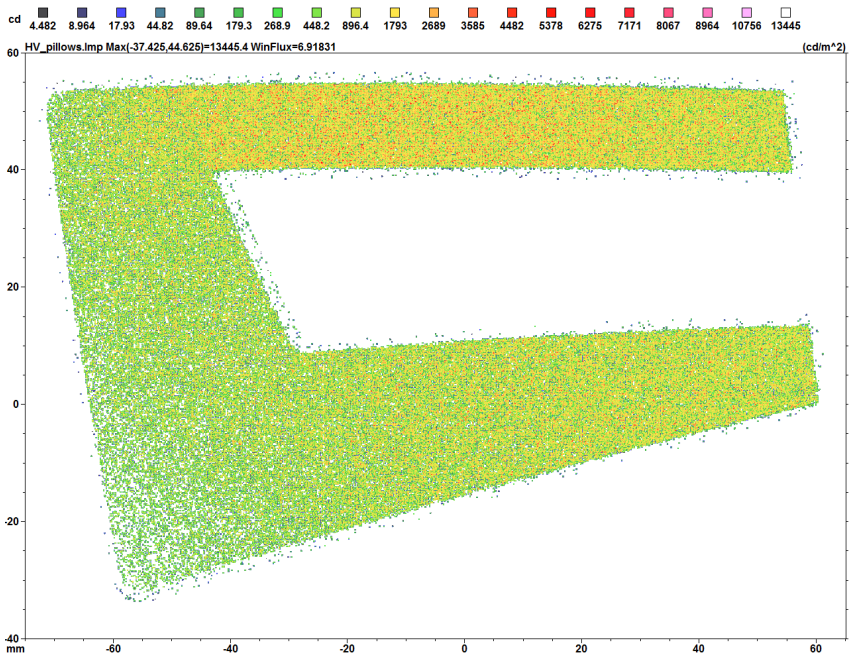

Figure 102: Lit appearance of pillows optics on B surface of Milky filter without any rotation

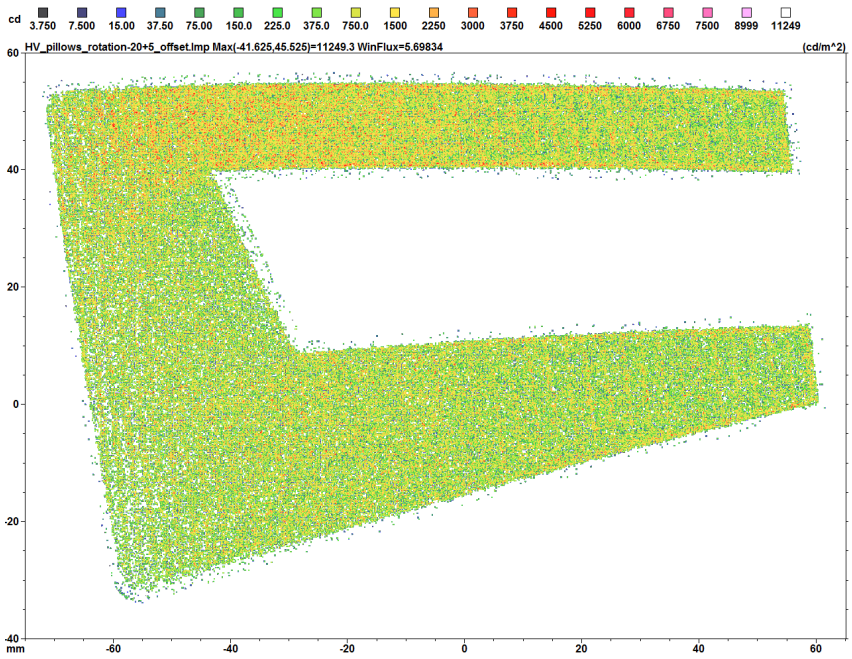

Figure 103: Lit appearance of pillows optics on B surface of Milky filter with rotation of pillows

In figure 104 is shown lit appearance created in software LuxRender. According to these figure, homogeneity of lit appearance is destroyed after using pillows optics on entire surface of Milky filter. For comparison, between different materials is also shown lit appearance of the transparent material (figure 105).

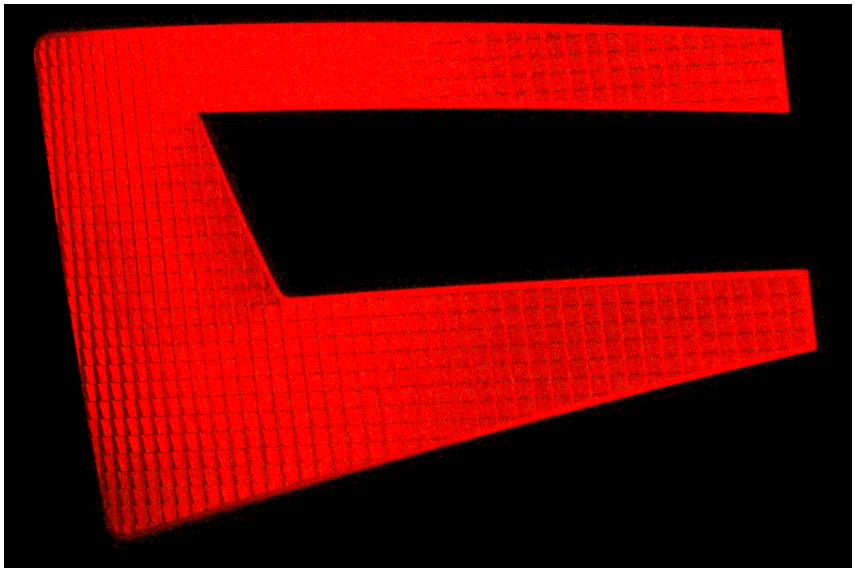

Figure 104: Lit appearance of pillows optics on B surface of Milky filter without any rotation

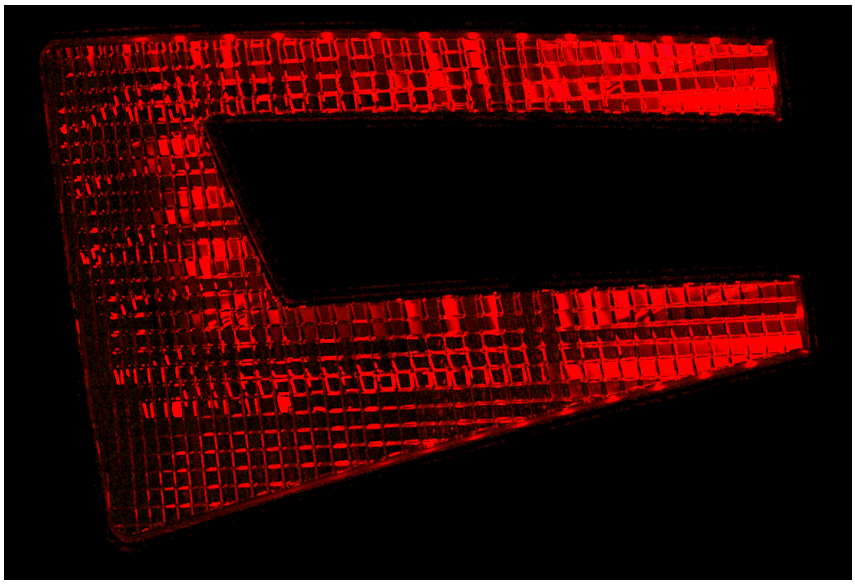

Figure 105: Lit appearance of pillows optics on B surface of Milky filter with rotation of pillows

In this subsection, I have described process of simulations where I was looking for a suitable optical system, which allow align the light to the required direction. I have decided for the pillows optics placed on entire B surface of Milky filter. In compliance with the iso candela maps shown in figures 96, 97, 98, 99, 101, it is possible to regulate light to the required direction by this optical system. However, from the lit appearances shown in figures 103, 104, 105 is clear that after using optical element on the Milky filter is very poor the homogeneity of the emitted light. Therefore the result from this simulation is following: although it is possible to align the light to the required direction, it has very large effect on homogeneity of emitted light, so the lamp does not meet the stylistic and aesthetic function. Due to this reason, it is not appropriate to use optical element on surfaces of Milky filter.

Conclusion

The aim of this thesis was to study new progressive material used in automotive industry, namely Milky material. The optical properties of this material are necessary to study closely before its using in automotive lighting.

The first part of this thesis comprises of the theoretical background which is necessary in order to understand the field of the automotive industry. Particular chapters in this part are dedicated to the fundamental optical principles related to the automotive lighting. I have described in detail a theoretical background of Milky material and gradually I have got to the basic phenomena of this material such as Volume scattering. Major part of the theory deals with the description of Geometrical optics since the dimensions of structures which interact the light in the automotive lighting application are much larger compared to the wavelength of the light. Within the theoretical part I have also described some new progressive technologies used in the automotive lighting. As results from the theoretical part of this thesis, the optical properties of the transparent material can be described by Geometrical optics. However, more complicated phenomena, namely Volume scattering has to be used in order to describe the optical properties of Milky material.

The practical part of this thesis is divided into two main simulations. The first point of the practical part was to perform a simulation with comparison of the optical properties of the individual elements made from Milky and transparent materials. Gradually, I have tested three types of the optical elements (flutes, optical pillows and simple prism) which were situated on the filter of simulated geometry. The aim of this simulation was to align the light to the visibility -80 ° on iso candela map with this optical element and to meet the standard ECE 7 for rear-right tail lamp. From the simulations is obvious that the most appropriate optical element for solving this problem was simple prism situated on B surface of Milky filter. Another optical elements were not able to align the light to the angle -80 °. However, on these elements were demonstrated optical properties of the individual materials and some differences between them. From the results is obvious that whereas optical elements made from the transparent material just refract the light, optical elements made from Milky material in addition spread the light much more uniformly. According to the results from the simulations, it is possible to align the light to the required direction with optical elements made from Milky material. Otherwise, lit appearances from the simulations indicate that positioning of any elements on Milky filter significantly impairs homogeneity of the emitted light.

Another point of the practical part was to propose an optical system which would be able to align the light to the required direction, specifically move to maximal intensity into point H-V on the iso candela map. Special optical elements (pillows optics) situated on the entire inner surface of Milky filter was used in order to meet this purpose. As well as the previous simulation, it is also possible to regulate light to the specific direction by using this kind of the optical elements. However, using additional optics on Milky filter has very large effect on

homogeneity of the emitted light as well as in previous situation.

On the basis of results obtained from this thesis is evident that the optical elements which are situated on Milky filter allow to align the light to the required direction. However, placement of the optical elements on any surface of Milky filter has a major effect on homogeneity of the emitted light. Thus, conclusion of this thesis consists in a fact that it is not proper to place any optical element on filter made from Milky material due to the increasing requirements on aesthetic and stylistic function of the automotive lamps.

References

[1] Altuglas, *Lighting solutions for your innovations*, In: Altuglas [online], [2016-03-31]. http://www.altuglas.com/export/sites/altuglas/.content/medias/downloads/literature/Altuglas-resins-lighting-innovation-GB-brochure.pdf.

[2] Plastix Word, *Better with a diffusing polymer.* 2013 [2016-03-31], [online] http://www.plastix-world.com/better-with-a-diffusing-polymers/

[3] KANEMITSU, Akiyoshi., *Light Diffuser Plates for LCD-TV Backlight Systems*, In: SUMITOMO CHEMICAL [online], [2016-03-31]. http://www.sumitomo-chem.co.jp/english/rd/report/theses/docs/20070100_sv7.pdf/

[4] PLEXIGLAS® LED white 0V200., *Product Information.*, [2016-03-31],[online]. http://www.plexiglas-polymers.com/sites/dc/Downloadcenter/Evonik/Product/PLEXIGLAS-Molding-Compounds/en/Product-Information

[5] Altuglas, *Altuglas Blocks: LED Letters*, [2016-04-24], [online] http://www.sunclear.fr/pdf/20110228-altuglas-blocks-led-letterspdf.pdf

[6] Altuglas, *Altuglas, lighting solutions for your innovations.*, [2016-03-31], [online]. http://www.altuglas.com/export/sites/altuglas/.content/medias/downloads/literature/Altuglas-resins-lighting-innovation-GB-brochure.pdf

[7] WANTJER, Malte., *Automotive – Light Sources: Presentation to the lecture incoherent light sources.* In: FH Munster: University of Applied Sciences [online]. [2016-03-31]. https://www.fh-muenster.de/fb1/downloads/personal/juestel/juestel/Automotive_Light_Sources_MalteWantjer_.pdf

[8] Varroc Lighting Systems, *Rear Lamps.* [online], [2016-04-24], varroclighting.com/rear-lamps-81.htm

[9] Svítidla a světelné přístroje., *Současnost a budoucnost automobilového osvětlení*, [online], [2015-05-06], http://www.odbornecasopisy.cz/res/pdf/44730.pdf

[10] OSRAM, *OLED (organic LED): A top lighting trend for automotive lighting.*, 2013, [online], [2016-02-23], http://www.osram.com/osram_com/news-and-knowledge/automotive-special/trends-in-automotive-lighting/oled-in-automotive-lighting/index.jsp

[11] OLED-info, *BMW's M4 Concept Iconic Light uses ORSAM's OLED panels*, [online], [2016-02-23] http://www.oled-info.com/bmws-m4-concept-iconic-light-uses-orsams-oled-panels

[12] OSRAM, *Laser light for headlights: latest trend in car lighting.*, [online], [2016-02-23], http://www.osram.com/osram_com/news-and-knowledge/automotive-special/trends-in-automotive-lighting/laser-light-new-headlight-technology/index.jsp

[13] HABEL, Jiří., *Světlo a osvětlování*, Praha: FCC Public, 2013. ISBN 978-80-86534-21-3.

[14] Tucson, *Radiometry and photometry FAQ.*, Internet archive [online], 2003 [2016-02-24]. http://web.archive.org/web/20120912080047/http://www.optics.arizona.edu/palmer/rpfaq/rpfaq.htm

[15] EDU.photonics.com, *Photometry: The Answer to How Light Is Perceived.*, [online], [2016-02-24], http://www.photonics.com/EDU/Handbook.aspx?AID=25119

[16] Petr Ferbas., *Optika a její využití v automobilovém osvětlení.*, In: Excom.vsb.cz [online]. [2016-04-25]. http://excom.vsb.cz/images/files/2014_9TES/OPTIKA_VSB_2014_ESF.pdf

[17] Regulation No. 37., *Uniform provisions concerning the approval of filament lamps for use in approved lamp units of power-driven vehicles and of their trailers.* In: . Revision 8. UNITED NATIONS, 2015. http://www.unece.org/fileadmin/DAM/trans/main/wp29/wp29regs/updates/R037r8e.pdf

[18] BASS, Michael a Virendra N MAHAJAN., *Handbook of optics. 3rd ed.* New York: McGraw-Hill, 2010. ISBN 978-007-1633-130.

[19] SALEH, Bahaa E a Malvin Carl TEICH., *Fundamentals of photonics.*, New York: Wiley, c1991. ISBN 04-718-3965-5.

[20] MAHAJAN, Virendra N., *Fundamentals of geometrical optics.* Bellingham: SPIE Press, 2014. ISBN 978-0-8194-9998-1.

[21] Addendum 6: Regulation No. 7. *Uniform provisions concerning the approval of front and rear position lamps, stop-lamps and end-outline marker lamps for motor vehicles (except motor cycles) and their trailers.* Revision 6. UNITED NATIONS, 2012. https://www.unece.org/fileadmin/DAM/trans/main/wp29/wp29regs/updates/R007r6e.pdf

A Electronic appendix

The following annexes are part of the CD.

Datasheet of used LED

CATpart of simulated geometry

Iso candela maps

Lit appearances